

Annual Report  
Materials Science with Muon Spin Rotation  
Virginia State University  
Petersburg, VA 23803

IN-72-CK

111111

(1+6)

142715

Supported by NASA Grant NAG-1-416  
Report Period: 3/1/87 - 2/29/88

P-92

PERIOD

(NASA-CR-182891) MATERIALS SCIENCE WITH  
MUCN SPIN ROTATION Annual Report, 1 Mar.  
1987 - 29 Feb. 1988 (Virginia State Univ.)  
92 p

CSCI 20L

N88-24242  
--THRU--  
N88-24248  
Unclas  
0142715

63/72

Annual Report  
Materials Science with Muon Spin Rotation  
Virginia State University  
Petersburg, VA 23803

Supported by NASA Grant NAG-1-416  
Report Period: 3/1/87 - 2/29/88

During the twelve-month period March 1, 1987 through February 29, 1988 the focus of activity in the MSMSR program was muon spin rotation studies of superconducting materials, in particular the new high-T<sub>c</sub> materials and the heavy-fermion materials CeCu<sub>2.1</sub>Si<sub>2</sub>.

A set of MuSR experiments was done at the Alternating Gradient Synchrotron of Brookhaven National Laboratory in May 1987. Three materials were studied: (1) the high-T<sub>c</sub> superconductor YBa<sub>2</sub>Cu<sub>3</sub>O<sub>7</sub>, (2) an oxygen-depleted variant on the "parent" compound to La<sub>1.85</sub>Sr<sub>0.15</sub>CuO<sub>4</sub>, La<sub>2</sub>CuO<sub>4-y</sub>, and (3) the heavy-fermion superconductor CeCu<sub>2.1</sub>Si<sub>2</sub>.

The data obtained on YBa<sub>2</sub>Cu<sub>3</sub>O<sub>7</sub> were combined with data obtained on La<sub>1.85</sub>Sr<sub>0.15</sub>CuO<sub>4</sub> in February 1987 in a paper, "Systematic Variation of Magnetic-field Penetration Depth in High-T<sub>c</sub> Superconductors Studied by Muon Spin Relaxation", which has been submitted to Physics Review B for publication. It is included as Appendix A to this report.

The data obtained on La<sub>2</sub>CuO<sub>4-y</sub> are presented in a paper which was published in Physical Review Letters on August 31, 1987. This is included as Appendix B to this report. A further comparison of these data with neutron scattering results was reported by our colleague Y. J. Uemura at the Interlachen HTSC-M<sup>2</sup>S Conference in February 1988. This paper, which will appear in the conference proceedings, is also included in this report as Appendix C.

The director spent the period August 1-6, 1987 at the TRIUMF laboratory in Vancouver, B.C., working on a MuSR study of YBa<sub>2</sub>Cu<sub>3</sub>O<sub>7-y</sub>, which was found to be antiferromagnetic below about 220K, similar to La<sub>2</sub>CuO<sub>4-y</sub>. These results were published in the March 14, 1988 issue of Physical Review Letters and are included in this report as Appendix D.

The May 1987 study of CeCu<sub>2.1</sub>Si<sub>2</sub> indicated the simultaneous presence of superconductivity and static magnetic ordering in this material below about 0.8K. Further MuSR studies with a helium-dilution refrigerator were clearly needed, so the director, along with two colleagues from the College of William and Mary (W. J. Kossler and X. H. Yu) and Y. J. Uemura of BNL went to the Swiss Institute for Nuclear Research in November 1987 to study CeCu<sub>2.1</sub>Si<sub>2</sub> in the MuSR low-temperature facility there.

The phenomenon observed at BNL was confirmed and the magnetic ordering appears to be a spin glass. These results are detailed in a paper which has been submitted to Physical Review Letters and is included here as Appendix E. A shortened and revised version of this paper was presented at the Interlaken HTSC-M<sup>2</sup>S meeting by Y. J. Uemura. It is included here as Appendix F. The travel to Switzerland was supported by the National Science Foundation.

Apart from superconductors, we also continued to analyze data taken during earlier experimental runs on metal hydrides. A paper on "Muon Motion in Titanium Hydride" is being submitted to Physical Review B and is included here as Appendix G.

The director spent the periods July 11-August 1 and August 12-September 3, 1987 at the Los Alamos Meson Physics Facility (LAMPF) working on two nuclear physics experiments, a search for eta-mesic nuclei, and a study of nuclear pion charge-exchange reactions at rest. His travel was supported by a National Science Foundation grant administered by the College of William and Mary. VSU graduate student Norman Fuqua (since graduated) participated in the July run.

A paper based upon a December 1986 search for eta-mesic nuclei done at the Brookhaven AGS has been accepted for publication in Physical Review Letters. It is included in this report as Appendix H.

A long set of MuSR experiments at BNL began in February 1988 and continued into May 1988 (which explains the lateness of this annual report). A variety of high-T<sub>c</sub> materials were studied, including YBa<sub>2</sub>Cu<sub>3-x</sub>Co<sub>x</sub>O<sub>7</sub>. These data will be described in the next six-month report.

Lucian R. Goode, Jr., who did his thesis research on MuSR studies of iron alloyed with gold, dysprosium and tantalum, received the M. S. degree in physics in May 1987. Norman Fuqua wrote his thesis on inelastic scattering of polarized protons from <sup>12</sup>C (done at Los Alamos) and received the M. S. degree in July 1987. Li-Tai Song has passed the orals on his thesis, "The Surface Muon Beam at Brookhaven National Laboratory" and should receive the M. S. degree in July 1988. Nana Adu has passed the orals on his thesis, "A Muon Spin Rotation Study of Zirconium Hydride", and should also receive the M. S. degree in July 1988. A senior physics major, Michael R. Davis, who worked extensively on this research program, graduated magna cum laude from VSU in July 1987.

The director gave four talks on the studies of superconducting materials done at BNL, TRIUMF, and SIN during this reporting period. They were presented at the Virginia Academy of Science meeting in Norfolk in May 1987, at a MuSR colloquium held at the Los Alamos Meson Physics Facility in August 1987, at a NASA workshop held at the NASA Langley Research

Center in January 1988, and at a meeting of the VSU Society of Physics Students, also held in January 1988. A presentation was planned for the Virginia Academy of Science meeting to be held in Charlottesville in May 1988.

The director continues to serve on the board of trustees of the Southeastern Universities Research Association, which is building the Continuous Electron Beam Accelerator Facility in Newport News, VA, and which operates the SURANet computer network. In December 1987 he was appointed to the board of directors of the Virginia Research Network, and in May 1987 he was appointed to the Governor's Ad Hoc Committee on the Superconducting Super Collider.

A temperature controller and a CAMAC crate controller, both ordered during the SSPRI grant period, arrived during the summer of 1987 and have been installed in the MuSR rig at BNL. An 8-MHz 80287 math chip for the IBM PC/XT has been installed and is operating.

Dr. Robert I. Grynszpan, the co-investigator of this research program, was in residence at VSU between October 28 and November 14, 1987. He worked with Dr. Min Namkung of NASA Langley on magnetoacoustic measurements of fatigue in metals during his visit. These results will be included in the next report. A student of Dr. Grynszpan from the University of Paris, Patrick Langlois, is expected to visit VSU as an exchange student during the summer of 1988. He will work with Dr. Namkung at NASA Langley on further magnetoacoustic measurements of fatigue in metals.

The report period of March 1, 1987 to February 29, 1988 saw the development of muon spin rotation into perhaps the best technique for measuring the microscopic properties of high-Tc and heavy-fermion superconductors. The coming year is full of promise for continued studies in these areas, as well as the more traditional areas which utilize the muon probe, such as metal hydrides and magnetism.

We appreciate the support of NASA, and the collaboration of scientists from William and Mary, Brookhaven National Laboratory, George Mason University, and NASA Langley, all of which have been vital to the success of this program.

Carey E. Stronach  
Director  
June 3, 1988

APPENDIX A

Systematic Variation of Magnetic-field Penetration Depth  
in High- $T_C$  Superconductors Studied by Muon Spin Relaxation

Y.J. Uemura <sup>1)</sup>, V.J. Emery <sup>1)</sup>, A.R. Moodenbaugh <sup>1)</sup>, M.Suenaga <sup>1)</sup>, D.C. Johnston <sup>2),a)</sup>  
A.J. Jacobson <sup>2)</sup>, J.T. Lewandowski <sup>2)</sup>, J.H. Brewer <sup>3)</sup>, R.F. Kiefl <sup>3)</sup>, S.R. Kreitzman <sup>3)</sup> /  
G.M. Luke <sup>3)</sup>, T. Riseman <sup>3)</sup>, C.E. Stronach <sup>4)</sup>, W.J. Kossler <sup>5)</sup>, J.R. Kempton <sup>5),b)</sup>  
X.H. Yu <sup>5)</sup>, D. Opie <sup>5)</sup>, H.E. Schone <sup>5)</sup>

- 1) *Brookhaven National Laboratory, Upton, New York 11973*
- 2) *Corporate Research Laboratories, Exxon Research and Engineering Co., Annandale, New Jersey 08801*
- 3) *TRIUMF and Department of Physics, University of British Columbia, Vancouver, British Columbia, V6T 2A3, Canada*
- 4) *Virginia State University, Petersburg, Virginia 23803*
- 5) *College of William and Mary, Williamsburg, Virginia 23185*

ABSTRACT

The muon spin relaxation rate  $\sigma$  has been measured in the high- $T_C$  superconductors  $YBa_2Cu_3O_x$  for  $x = 6.66, 6.95, 7.0$ , and  $La_{1.85}Sr_{0.15}CuO_4$  in transverse external magnetic fields  $1 \sim 4kG$ . We find a simple relation which connects the transition temperature  $T_C$ , the magnetic-field penetration depth  $\lambda_L$ , the carrier concentration  $n_s$ , and the effective mass  $m^*$  as  $T_C \propto \sigma \propto 1/\lambda_L^2 \propto n_s/m^*$ . The linear dependence  $T_C \propto n_s/m^*$  suggests a high energy scale for the coupling between superconducting carriers.

The discovery<sup>1,2</sup> of the layered Oxide high- $T_C$  superconductor systems  $La_{2-y}Sr_yCuO_4$  and  $YBa_2Cu_3O_7$  has triggered extensive experimental activity<sup>3</sup> and renewed theoretical interest<sup>4,5</sup> in the search for a novel mechanism for superconductivity. Muon Spin Relaxation ( $\mu$ SR) is a direct method<sup>6</sup> for measuring magnetic-field penetration depth in superconductors<sup>7</sup>.  $\mu$ SR has been applied to the high- $T_C$  oxide superconductors<sup>8-11</sup> and related antiferromagnets<sup>12,13</sup>. Because of recent technological development in sample preparation, it has now become possible<sup>14</sup> to study single-phase specimens with the oxygen concentration controlled to within  $\pm 0.02$  per formula unit (/f.u.). In this paper, we present  $\mu$ SR measurements on  $YBa_2Cu_3O_x$  superconductors with averaged oxygen concentrations  $x = 7.0, 6.95, \text{ and } 6.66$  /f.u.. We combine these results with the earlier work<sup>9</sup> on  $La_{1.85}Sr_{0.15}CuO_4$ , and focus on the systematic dependence of the observed muon relaxation rate  $\sigma$  and the derived penetration depth  $\lambda_L$ . The results indicate that the superconducting transition temperature  $T_C$  is approximately proportional to the superconducting carrier concentration  $n_s$ , divided by the effective mass  $m^*$ . We discuss the implication of this relation on energy scales of the coupling between the carriers.

The sintered pellet specimen of  $YBa_2Cu_3O_7$  was prepared using a method described in ref. 15. The powder specimens of  $YBa_2Cu_3O_{6.95}$  and  $YBa_2Cu_3O_{6.66}$  were prepared by using another method described in ref. 14. which reports Meisner effect and susceptibility measurements on a series of  $YBa_2Cu_3O_x$  specimens ranging from  $x = 6.0$  to  $7.0$ . The specimens with  $x \geq 6.5$  show superconductivity. The  $\mu$ SR experiments on  $YBa_2Cu_3O_7$  were performed at the AGS muon channel of Brookhaven National Laboratory with a transverse external magnetic field  $H_{ext}$  of  $1 \text{ kG}$  applied perpendicular to the initial direction of muon spin polarization. The measurements on  $YBa_2Cu_3O_{6.95}$  and  $YBa_2Cu_3O_{6.66}$  were

carried out at the M15 muon channel of TRIUMF (Vancouver) with  $H_{ext} = 4kG$ . In both cases, the data were taken by cooling the specimen in external field from  $T \geq T_C$  to lower temperatures.

In the transverse-field  $\mu^+SR$  experiments, one observes the decay time histogram of positive muons stopped in the specimen

$$N(t) \propto \exp(-t/\tau_\mu)[1 + AG_x(t)\cos(\omega_\mu t)], \quad (1)$$

where  $\tau_\mu$  is the muon lifetime  $2.2 \mu\text{sec}$ ,  $A$  is the initial precession asymmetry,  $\omega_\mu$  is the muon precession frequency, and the relaxation function  $G_x(t)$  represents the time evolution of the muon spin polarization. At all measuring temperatures ( $5.0K \leq T \leq 300K$ ), the observed precession amplitude  $A$  indicates that within experimental error all the muons stopped in the specimen contribute to the precession signal. The frequency  $\omega_\mu$  was approximately equal to  $\gamma_\mu H_{ext}$  ( $\gamma_\mu = 2\pi \times 1.355 \times 10^4/Oe$  is the gyromagnetic ratio of  $\mu^+$ ) above  $T_C$ .  $\omega_\mu$  decreased slightly with decreasing temperature below  $T_C$ , due to the partial exclusion of the external field  $H_{ext}$  in the type II superconductors at  $H_{ext} \geq H_{c1}$ . For simplicity, here we assume a Gaussian shape for  $G_x(t)$ :

$$G_x(t) = \exp(-\frac{\sigma^2 t^2}{2}), \quad (2)$$

where  $\sigma$  is the muon spin relaxation rate.

Figure 1 shows the temperature dependence of  $\sigma$  obtained for the present  $YBa_2Cu_3O_x$  compounds together with the earlier results<sup>9</sup> on  $La_{1.85}Sr_{0.15}CuO_4$ . The very small values of  $\sigma$  observed in all the specimens above  $T_C$  can be accounted for by nuclear dipolar broadening. Combining this feature with the full amplitude for  $A$  and the reduction

of  $\omega_\mu$  below  $T_C$ , one can conclude that there is no static magnetic ordering in these superconducting specimens either above or below  $T_C$ . This aspect was confirmed in the zero-field  $\mu$ SR measurements on  $YBa_2Cu_3O_7$ . Below  $T_C$ , the value of  $\sigma$  increases rapidly with decreasing temperature. This is due to the inhomogeneity of the static local field at the muon site in the type-II superconducting state where  $H_{ext}$  penetrates as a lattice of flux vortices. We notice here that the four different specimens in Fig. 1 have reasonably similar shapes for the curvature of the temperature dependences  $\sigma(T)$ . This implies that  $T_C$  is approximately proportional to  $\sigma(T \rightarrow 0)$ , as demonstrated in Fig. 2 for the four different specimens.

Pincus et al.<sup>16</sup> used the London equation to calculate the distribution of magnetic fields in the vortex state, and obtained the second moment

$$\sqrt{\langle \Delta H^2 \rangle} \cong \frac{\phi_0}{\lambda_L^2 \sqrt{16\pi^3}} \quad (3)$$

with the flux quanta  $\phi_0$ , for the square lattice of the vortex when the second moment becomes independent of the external field  $H_{ext}$ , i.e., when  $\lambda_L$  is comparable to or greater than the distance between adjacent vortices. The present condition with  $H_{ext} = 1 \sim 4kG$  satisfies this criterion. For a triangular lattice, one needs to multiply<sup>10</sup> a factor of 0.93 to the right hand side of eq. (3). Then, one can deduce the value of the penetration depth  $\lambda_L$  directly from the observed relaxation rate  $\sigma$  which corresponds to  $\gamma_\mu \sqrt{\langle \Delta H^2 \rangle}$ . Figure 3 shows the temperature dependence of  $\lambda_L$  thus obtained for the triangular vortex lattice. The values for  $\lambda_L(T \rightarrow 0)$  are listed in Table 1. In the field-cooled measurements, the density of the magnetic flux is kept almost constant above and below  $T_C$ . If one changes the external field in the superconducting state, in contrast, the flux vortices have

to move within the sample to change the spatial flux density, and thus the experimental results become sensitive to the flux pinning<sup>17</sup>. Therefore, it is important to measure the penetration depth in the field-cooled condition, as in the present experiment.

In actual systems, we noticed that the functional form of  $G_x(t)$  is somewhat in between Gaussian and exponential. This is due to the complicated distribution of magnetic fields for the vortex lattice as well as to the effect of anisotropy on the penetration depth  $\lambda_L$ . Correcting for the former effect would reduce the resulting values of  $\lambda_L$  by about 30 %. For the case of maximum anisotropy where the penetration depth  $\lambda$  in the soft direction ( $H_{ext}$  applied parallel to the  $CuO$  plane) is infinite, Celio *et al.*<sup>18</sup> find that the value of  $\lambda$  for  $H_{ext} \perp \{CuO \text{ plane}\}$  to be about half the powder averaged value. These corrections make it difficult to deduce the absolute values of  $\lambda_L$  accurately. However, we stress here that the relation  $\sigma \propto 1/\lambda_L^2$  holds for any of the above calculations. Therefore, the systematic and temperature variations of  $\lambda_L$  can be discussed based on Figs. 1 and 3.

The London penetration depth  $\lambda_L$  is given as a function of effective mass  $m^*$  and the carrier density  $n_s$  as

$$\lambda_L = \sqrt{\frac{m^* c^2}{4\pi n_s e^2}}, \quad (4)$$

Combining this with the relation  $\sigma = \gamma_\mu \sqrt{\langle \Delta H^2 \rangle}$ , eq.(3), and the approximate experimental result  $\sigma \propto T_C$ , we obtain a simple relation

$$\sigma \propto \frac{1}{\lambda_L^2} \propto \frac{n_s}{m^*} \propto T_C. \quad (5)$$

Thus, the transition temperatures  $T_C$  of the four different samples are simply proportional to the carrier concentration  $n_s$  divided by the effective mass  $m^*$  regardless of the crystallographic differences of the samples.

The relation  $T_C \propto n$  ( $n$ : normal-state carrier density) has been found by Hall constant and related measurements for  $La_{2-y}Sr_yCuO_4$  between  $y = 0 \sim 0.15$  (ref. 19) and  $YBa_2Cu_3O_x$  between  $x = 6.5 \sim 7.0$  (ref. 20). This linear relation can also be obtained in a calculation of the number of holes for a formula unit, assuming charge neutrality for  $La_2CuO_4$  and  $YBa_2Cu_3O_{6.4}$  and adding 1 hole for the substitution of  $Sr$  to  $La$  and 2 holes for additional oxygen per formula unit. These results suggest that the carrier concentration  $n_s$ , rather than the effective mass  $m^*$ , plays a major role in changing  $T_C$  in eq. 5. Indeed, the Pauli susceptibility at  $T \geq T_C$  or the Sommerfeld constant  $\gamma$  of the low temperature specific heat, which are proportional to  $m^*n^{1/3}$ , do not depend much on the differences in material<sup>21</sup>, supporting the above view point. The present work has shown that the linear relation holds for the superconducting carrier concentration  $n_s$ .

We now discuss the implications of the relation  $T_C \propto n_s/m^*$ . In the BCS theory<sup>22</sup> with the phonon-mediated coupling of electrons,  $T_C$  is given in the so-called weak coupling limit as

$$k_B T_C \sim 2\hbar\omega_D \exp\left(-\frac{2}{V D(\epsilon_f)}\right), \quad (6)$$

where  $k_B$  is the Boltzmann constant,  $\omega_D$  is the Debye frequency,  $V$  represents the effective attractive interaction, and  $D(\epsilon_f)$  is the density of states at the Fermi energy  $\epsilon_f$ . To obtain this equation, one assumes  $\epsilon_f \gg \hbar\omega_D$  and solves the secular equation by integrating the energy range of the coupling interaction  $0 \rightarrow \hbar\omega_D$ , which results in the pre-exponential factor  $\hbar\omega_D$ . It is difficult to reconcile the relation  $T_C \propto n_s/m^*$  with eq. (6), because  $D(\epsilon_f)$  does not depend on  $n$  in the 2-dimensional non-interacting electron gas. Recent single-crystal measurements<sup>23</sup> on  $H_{c2}$  and on the transport properties suggest a highly

2-dimensional character for the electron system. Moreover, the magnitude of the electron-phonon interaction  $V$ , inferred from the temperature dependence of linear resistivity in the normal state<sup>24</sup>, is too small to explain the high transition temperature in the standard phonon-mediated mechanism.

In contrast, when the energy scale of the attractive interaction which couples the carriers is larger than that of  $\epsilon_F$ , the energy integration in the secular equation runs over the range 0 to  $\epsilon_f$ . This would put, roughly speaking,  $\epsilon_f$  in the pre-exponential factor of eq. (6) instead of  $\hbar\omega_D$ . In a two-dimensional non-interacting electron gas, the Fermi energy  $\epsilon_f$  is proportional to the quantity  $n/m^*$ . Then one could expect the simple relation  $T_C \propto n_s/m^*$ . This argument works without essential change also for three dimensional systems where  $\epsilon_F \propto n^{2/3}/m^*$ . Thus, the relation  $T_C \propto n_s/m^*$  suggests a high energy scale of the interaction which mediates the coupling between superconducting carriers in high- $T_C$  superconductors. Such a high energy scale may be found in models based on the large transfer integral of a carrier between the oxygen and neighboring copper atoms<sup>5</sup>. The linear relation  $T_C \propto n_s$  is also expected in a resonating-valence-bond picture<sup>25</sup>.

We study the temperature dependence of  $\lambda_L$  with examples of  $YBa_2Cu_3O_{6.95}$  and  $YBa_2Cu_3O_{7.0}$ . The sharp changes of  $\sigma(T)$  near  $T_C$  observed for these samples suggest a good homogeneity in the oxygen concentration. As shown by the solid lines in Fig. 3, the experimental data agree well with the empirical formula<sup>22</sup>

$$\lambda_L(T) = \frac{\lambda_L(T=0)}{\sqrt{1 - (T/T_C)^4}}. \quad (7)$$

This result is consistent with earlier  $\mu$ SR works<sup>8,10</sup>, but disagrees with a recent bulk measurement<sup>26</sup>. Equation (7) is calculated for  $\lambda_L$  much smaller than the coherence length

$\xi$  by assuming an isotropic energy gap at the Fermi surface. For  $\lambda_L \gg \xi$ , the BCS theory<sup>22</sup> predicts that  $\lambda_L(T)$  increases more rapidly than eq. (7) with increasing temperature at  $T \leq 0.7T_C$ . The anomalous zeros of the energy gap at some point or line of the Fermi surface would change the theoretical curves for  $\lambda_L(T)$  to increase faster with increasing temperature in the low temperature region. Therefore, the present results suggest that the energy gap is predominantly finite.

In summary, based on the muon spin relaxation experiments, we have shown that the approximate proportionality  $T_C \propto n_s/m^*$  holds universally for different high- $T_C$  oxide superconductor systems. This feature suggests the high energy scale of the coupling between superconducting carriers.

This work is supported by the Division of Materials Sciences, US Department of Energy under contract 76-AC02-CH00016, the US National Science Foundation under DMR 8503223, NASA under NAG-1-416, and by the NSERC of Canada.

## REFERENCES

- a) present address: Department of Physics and AMES Laboratory (USDOE), Iowa State University, Ames, Iowa 50011.
- b) present address: TRIUMF, UBC, Vancouver, B.C., V6T 2A3, Canada.
1. G.J. Bednorz and K.A. Müller, *Z. Phys.* B64, 189 (1986).
  2. S. Uchida *et al.*, *Jap. J. Appl. Phys. Lett.*, 26, L1 (1987); C.W. Chu *et al.*, *Phys. Rev. Lett.* 58, 405 (1987); R.J. Cava *et al.*, *ibid.* 408; M.K. Wu *et al.*, *ibid.* 908 (1987)
  3. see, for example, papers published in *Phys. Rev. Lett.* 58, 59 (1987), *Phys. Rev.* B35, B36 (1987), and *Jap. J. Appl. Phys. Lett.* 26 (1987).
  4. P.W. Anderson, *Science* 235, 1196 (1987).
  5. V.J. Emery, *Phys. Rev. Lett.* 58, 2794 (1987).
  6. For general aspects of muon spin rotation, see proceedings of the four previous international conferences, *Hyperfine Interact.* 6, (1979); 8, (1981), 17 – 19, (1984); 31, (1986).
  7. A.T. Fiory *et al.* *Phys. Rev. Lett.* 33, 969 (1974); F.N. Gygax *et al.* *Hyperfine Interact.* 8, 623 (1981).
  8. G. Aeppli *et al.* *Phys. Rev.* B35, 7129 (1987).
  9. W.J. Kossler *et al.*, *ibid.* 7133 (1987).
  10. F.N. Gygax *et al.* *Europhys. Lett.* 4, 473 (1987).
  11. D.R. Harshman *et al.*, *Phys. Rev.* B36, 2386 (1987).
  12. Y.J. Uemura *et al.*, *Phys. Rev. Lett.* 59, 1045 (1987).

13. N. Nishida *et al.*, Jap. J. Appl. Phys. 26, L1856 (1987).
14. D.C. Johnston *et al.*, *Chemistry of High- $T_C$  Superconductors*, ACS Symposium Series Vol. 351, Chap. 14, ed. by D.L. Nelson, M.S. Whittingham and T.F. George, Am. Chem. Society, Washington DC. (1987), pp 136-151; A.J. Jacobson *et al.*, Phys. Rev. *B* (submitted).
15. R.J. Cava *et al.*, Phys. Rev. Lett. 58, 1676 (1987); D.E. Cox *et al.*, J. Phys. Chem. Solids, in press.
16. P.Pincus *et al.*, Phys. Lett. 13, 21 (1964).
17. some examples of the flux pinning effect can be seen in refs. 8 and 10. According to a private communication with A. Schenck,  $\mu$ SR data taken in the zero-field cooling procedure are significantly different from specimen to specimen, even for the same nominal chemical formula.
18. M. Celio, T.M. Riseman, J.H. Brewer, R.F. Kiefl and W.J. Kossler, unpublished.
19. M.W. Shafer *et al.*, Phys. Rev. *B*36, 4047 (1987).
20. H. Takagi, K. Kitazawa *et al.*, un published.
21. K. Kitazawa *et al.*, Jap. J. Appl. Phys. Lett. 26, L748, L751 (1987).
22. J. Bardeen, L.N. Cooper and J.R. Schrieffer, Phys. Rev. 108, 1175 (1957).
23. Y. Hidaka *et al.*, Jap. J. Appl. Phys. Lett. 26, L377; L726 (1987); T.R. Dinger *et al.*, Phys. Rev. Lett. 58, 2687 (1987); T.K. Worthington *et al.*, Phys. Rev. Lett. 59, 1160 (1987).
24. M. Gurevitch and A.T. Fiory, Phys. Rev. Lett. 59, 1337 (1987).

25. G. Baskaran *et al.*, Solid State Commun. 63, 973 (1987); P.W. Anderson *et al.*, Phys. Rev. Lett. 58, 2793 (1987).
26. J.R. Cooper *et al.*, Phys. Rev. B37, 638 (1988).

## FIGURE CAPTIONS

Fig. 1.

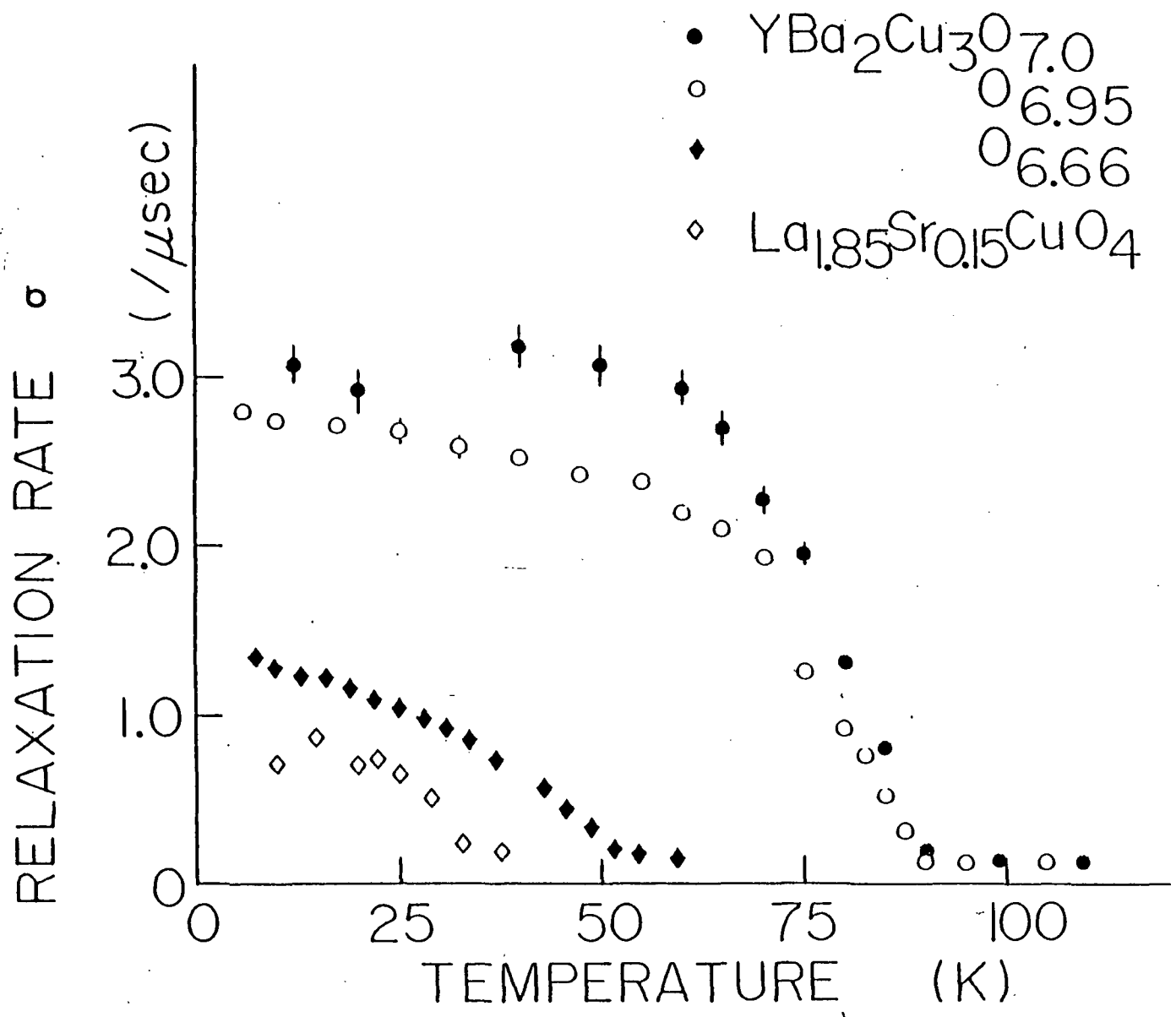
Temperature dependence of the relaxation rate  $\sigma$  of the muon spin polarization, as defined in eq. (2), observed in four different specimens of high- $T_C$  superconductors. Data on  $La_{1.85}Sr_{0.15}CuO_4$  and  $YBa_2Cu_3O_7$  were obtained in a transverse external magnetic field of 1 kG, while the measurements on the other two specimens were performed with a field of 4 kG.

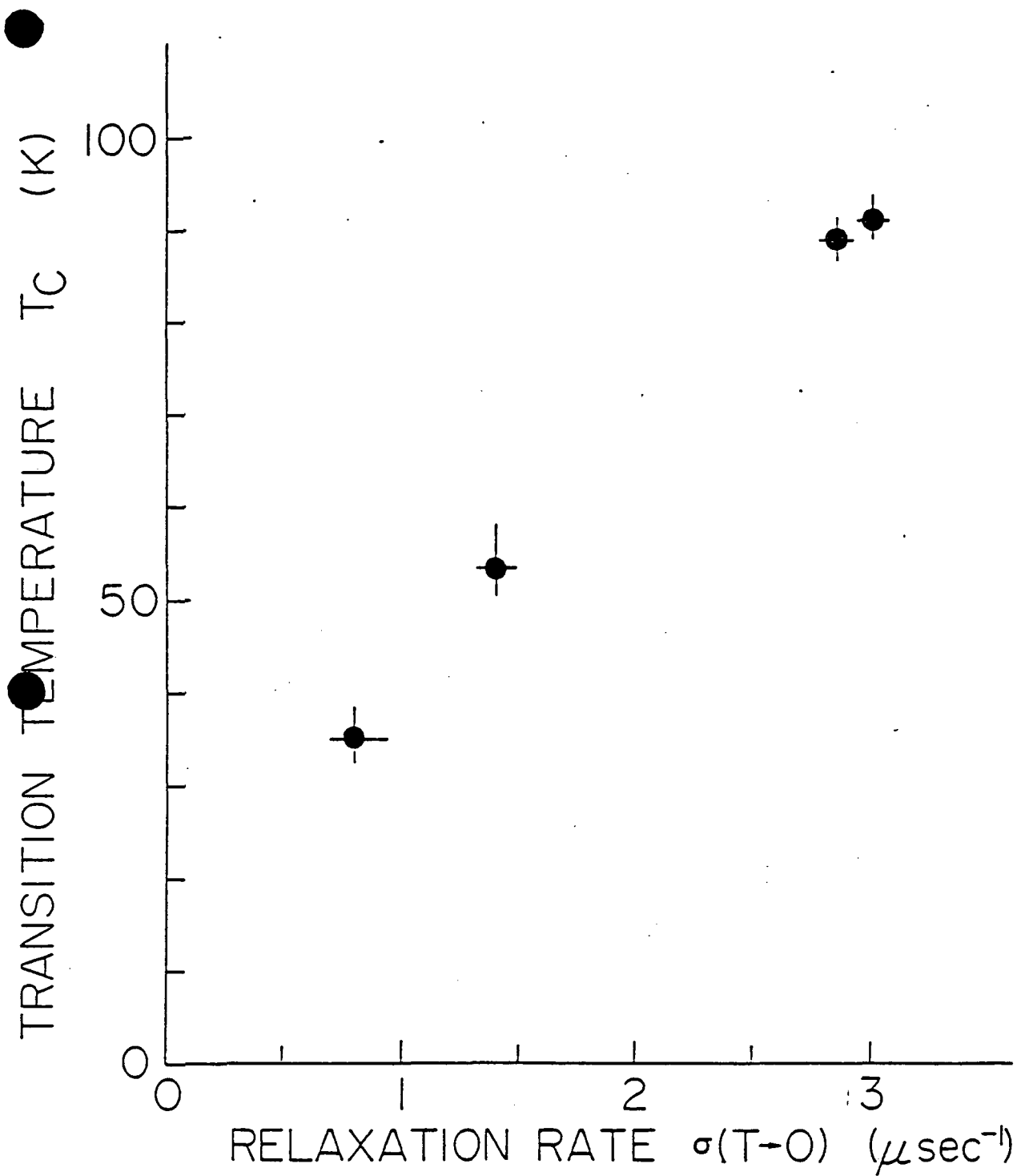
Fig. 2

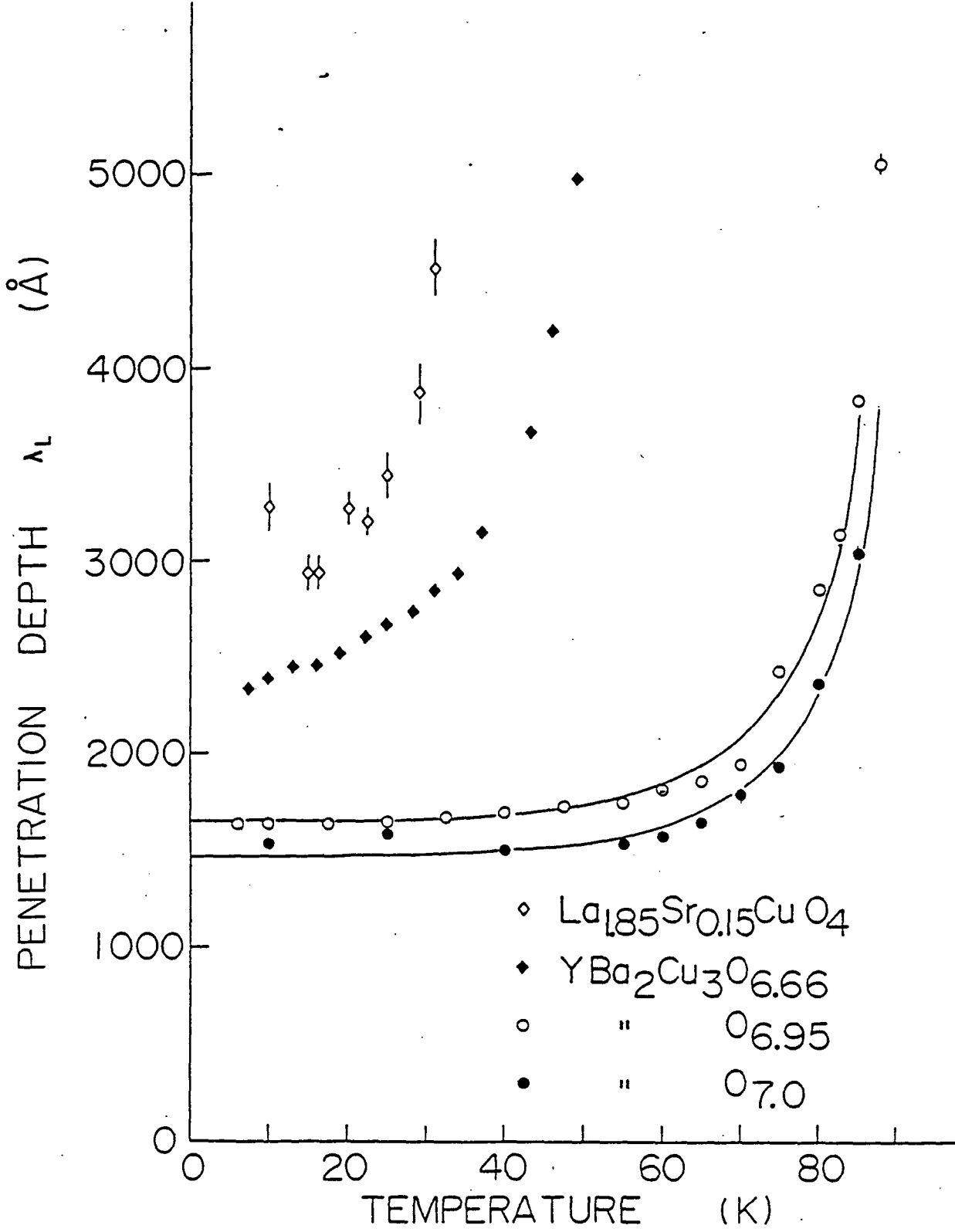
Superconducting transition temperature  $T_C$ , as determined by the  $\mu$ SR measurement, plotted versus the values of the muon relaxation rate  $\sigma$  at  $T \rightarrow 0$  for the four different specimens of high- $T_C$  superconductors.

Fig. 3

Temperature dependence of the magnetic field penetration depth  $\lambda_L$  derived from the muon spin relaxation rate shown in Fig. 1.  $\lambda_L$  was calculated using a simple approximation for the triangular vortex lattice as described in the text. The solid lines represent fits of the data to eq. 7, with  $\lambda_L(T = 0) = 1656 \text{ \AA}$  and  $T_C = 89.9 \text{ K}$  for  $YBa_2Cu_3O_{6.95}$ , and  $\lambda_L(T = 0) = 1472 \text{ \AA}$  and  $T_C = 91.1 \text{ K}$  for  $YBa_2Cu_3O_{7.0}$ .







APPENDIX C

Comparison between Muon Spin Rotation and Neutron Scattering Studies  
on the 3-Dimensional Magnetic Ordering of  $\text{La}_2\text{CuO}_{4-y}$

Y.J. Uemura<sup>1</sup>, W.J. Kossler<sup>2</sup>, J.R. Kempton<sup>2,4</sup>, X.H. Yu<sup>2</sup>, H.E. Schone<sup>2</sup>, D. Opie<sup>2</sup>  
C.E. Stronach<sup>3</sup>, J.H. Brewer<sup>4</sup>, R.F. Kiefl<sup>4</sup>, S.R. Kreitzman<sup>4</sup>, G.M. Luke<sup>4</sup>, T. Riseman<sup>4</sup>  
D.Ll. Williams<sup>4</sup>, E.J. Ansaldo<sup>5</sup>, Y. Endoh<sup>6</sup>, E. Kudo<sup>6</sup>, K. Yamada<sup>6</sup>, D.C. Johnston<sup>7,a</sup>  
M. Alvarez<sup>7</sup>, D.P. Goshorn<sup>7</sup>, Y. Hidaka<sup>8</sup>, M. Oda<sup>8</sup>, Y. Enomoto<sup>8</sup>, M. Suzuki<sup>8</sup>, T. Murakami<sup>8</sup>

1 Brookhaven National Laboratory, Upton, New York 11973, USA

2 College of William and Mary, Williamsburg, Virginia 23185, USA

3 Virginia State University, Petersburg, Virginia 23803, USA

4 TRIUMF and University of British Columbia, Vancouver, British Columbia, V6T 2A3,

Canada

5 University of Saskatchewan, Saskatoon, Saskatchewan, S7N 0W0, Canada

6 Tohoku University, Sendai 980, Japan

7 Corporate Research Laboratories, Exxon Research and Engineering Co., Annandale,

New Jersey 08801, USA

8 NTT Electrical Communications Laboratories, Tokai, Ibaraki 319-11, Japan

ABSTRACT

Muon spin rotation and neutron scattering studies on powder and single-crystal specimens of  $\text{La}_2\text{CuO}_{4-y}$  are compared. The apparent difference between the muon and neutron results for the ordered moment in the antiferromagnetic state is interpreted as the signature of increasingly short-ranged spatial spin correlations with increasing oxygen content.

(submitted to the Interlaken HTSC-M<sup>2</sup>S Conference, February, 1988)

It has been known<sup>1</sup> that the magnetic properties of the antiferromagnetic compound  $La_2CuO_{4-y}$  depend sensitively on small differences in the oxygen content  $y = 0 \sim 0.03$ . The input of  $O^{2-}$ , equivalent to the substitution of  $Sr^{2+}$  for  $La^{3+}$ , removes electrons and creates holes in the system, and suppresses the 3-dimensional antiferromagnetic ordering. To study this phenomenon with direct microscopic magnetic probes, experiments were performed using the muon spin rotation ( $\mu$ SR) (ref. 2) and neutron scattering<sup>3</sup> techniques. In this paper we present new  $\mu$ SR data obtained at TRIUMF on a single-crystal and several powder specimens, compare the muon and neutron results, and discuss their implications.

Figure 1 shows the muon spin precession frequency  $\nu_\mu$  observed in zero field for four different powder specimens of  $La_2CuO_{4-y}$ .  $\nu_\mu$  is proportional to the static internal magnetic field at the muon site from nearby ordered magnetic moments. Therefore, Fig. 1 represents the temperature and  $y$  variation of the ordered  $Cu$  moment  $S$ . It is remarkable that  $\nu_\mu(T \rightarrow 0) \propto S(T \rightarrow 0)$  changes only within about 15 % for the four specimens despite the large difference in the ordering temperatures  $T_N$  (from 300 K to 15 K). The ordered moment has also been measured by neutron scattering by Yamada *et al.* (ref. 3) on a few single crystal specimens of  $La_2CuO_{4-y}$ . Figure 2 shows the temperature variation of the sublattice magnetization  $M_s$  derived from the intensity of the 3-dimensional magnetic Bragg reflection. In contrast to the  $\mu$ SR results,  $M_s(T \rightarrow 0)$  decreases by more than a factor of 3 for the decreasing Néel temperatures of the specimens. In this respect,  $\mu$ SR and neutron measurements look inconsistent.

To study further details, we performed  $\mu$ SR measurements on a single-crystal specimen of  $La_2CuO_{4-y}$  (NTT No. 3 specimen in ref. 4, grown simultaneously in the same batch as sample No. 3 in Fig. 2 and in ref. 2). The neutron magnetic Bragg intensity was

measured on this crystal by Endoh *et al.*<sup>4</sup>, and the temperature variation was very close to the results shown for sample No. 3 in Fig. 2. The ordered moment estimated from the neutron study was about  $M_S(T \rightarrow 0) \sim 0.15\mu_B$ . Figure 3-(a) shows the muon spin precession frequency  $\nu_\mu$  measured on this specimen.  $\nu_\mu(T \rightarrow 0)$  is approximately equal to the values observed for the other powder specimens (Fig. 1), thus indicating that  $S(T \rightarrow 0)$  is not much different from the value  $0.5 \sim 0.6 \mu_B$  determined by the neutron experiment (Fig. 2) on the specimens with  $T_N \sim 300K$ .

We also performed  $\mu$ SR measurements in a weak transverse magnetic field of about 100G, and determined the volume fraction of the magnetically ordered part of the specimen as shown in Fig. 3-(b). The magnetic ordering takes place gradually between 200K and 100K, below which almost the entire volume of the specimen becomes antiferromagnetic. Lack of a sharp magnetic ordering is assumed to be due to the inhomogeneous spread of the oxygen concentration in the large single crystal specimen. Similarly, it is confirmed that the predominant volume fraction of the powder specimens orders magnetically below  $T_N$ . This rules out the explanation that the difference between muon and neutron results may be due to a non-ordered volume fraction of the specimens.

The difference between  $\mu$ SR and neutron results can be understood in the following way. The  $\mu^+$  is a point-like probe in real space, and the local field at a muon site is due mostly to its neighbouring *Cu* moments. Therefore, once the antiferromagnetic spin configuration becomes static ( $t \geq 1\mu\text{sec}$ ), even if the spatial correlation may be short ranged, the  $\mu^+$  sees the specimen to be almost perfectly antiferromagnetic. In contrast, the elastic magnetic scattering intensity of neutrons forms a peak in reciprocal space at the Bragg point only when the spatial 3-dimensional ordering is long ranged. Therefore, the

present results suggest that the magnetic ordering becomes more and more short-ranged with increasing oxygen content (i.e., with increasing number of holes), resulting in the decreasing Néel temperatures.

The closed-shell electron configuration of  $O^{2-}$  mediates the super-exchange antiferromagnetic coupling between adjacent  $Cu$  moments. When the introduction of a hole makes the oxygen to be  $O^{1-}$  (ref 5), the unpaired spin at the oxygen would mediate the effectively ferromagnetic coupling between neighbouring  $Cu$  moments. Therefore, the input of oxygen would create frustrated bonds<sup>6</sup> in the  $Cu - O$  plane, and thus help to destroy the long-ranged spin correlation. This picture provides a possible explanation for the present results. There are two possibilities for the short-ranged correlation: a) the randomness introduced within the  $Cu - O$  plane; and b) the cut-off of the spin correlation between different  $Cu - O$  planes. It is not possible to determine from the present work whether either or both of them take place. The neutron study of ref. 4 gives support to b) for the particular case of the specimen shown in Fig. 3.

By combining neutron and muon experiments, one can estimate the microscopic static moment to be  $S = 0.5 \sim 0.6\mu_B/Cu$ . This value is significantly smaller than the integer moment for spin 1/2, but it can be explained by the quantum spin reduction for the spin 1/2 2-d Heisenberg system obtained from the statistical-mechanics calculations<sup>7</sup>. A spin-density-wave state is another possibility to create the non-integer moment. From the present work alone, it is not possible to tell which is the case.

We are grateful for useful discussions with R.J. Birgeneau, V.J. Emery, G. Shirane and S.K. Sinha. This work is supported by the USDOE (DE-AC02-76CH00016), the US

NSF (DMR 8503223), NASA (NAG-1-416), the Canadian NSERC, and by the Japanese Ministry of Education, Culture and Science (Grant-in-Aid for Scientific Research).

## REFERENCES

- a) present address: Ames Laboratory (USDOE) and Department of Physics, Iowa State University, Ames, Iowa 50011, USA.
- 1 D.C. Johnston *et al.*, Phys. Rev. *B*36, 4007 (1987).
  - 2 Y.J. Uemura *et al.*, Phys. Rev. Lett. 59, 1045 (1987).
  - 3 K. Yamada *et al.*, Solid State Commun. 64, 753 (1987).
  - 4 Y. Endoh *et al.*, Phys. Rev. *B*, submitted (1988).
  - 5 V.J. Emery, Phys. Rev. Lett. 58, 2794 (1987), and references therein.
  - 6 A. Aharony *et al.*, preprint.
  - 7 see, for example, J. Oitmaa and D.D. Betts, Can. J. Phys. 56, 897 (1978), and references therein.

## Figure Captions

Fig. 1 Muon spin precession frequency  $\nu_\mu$  observed in zero external field on various sintered-powder specimens of  $La_2CuO_{4-y}$ .

Fig. 2 Sublattice magnetization  $M_s$  derived from the magnetic Bragg-peak intensity of neutrons on single-crystal specimens of  $La_2CuO_{4-y}$  by Yamada *et al.* (after ref. 3).

Fig. 3 (a) Muon spin precession frequency  $\nu_\mu$  measured in zero external field on the NTT No. 3 single-crystal of  $La_2CuO_{4-y}$ . (b) Volume fraction of the paramagnetic region of the specimen measured by muon spin rotation experiments in a weak transverse external magnetic field. It is shown that almost the entire volume of the sample orders magnetically below about  $T \sim 100K$ .

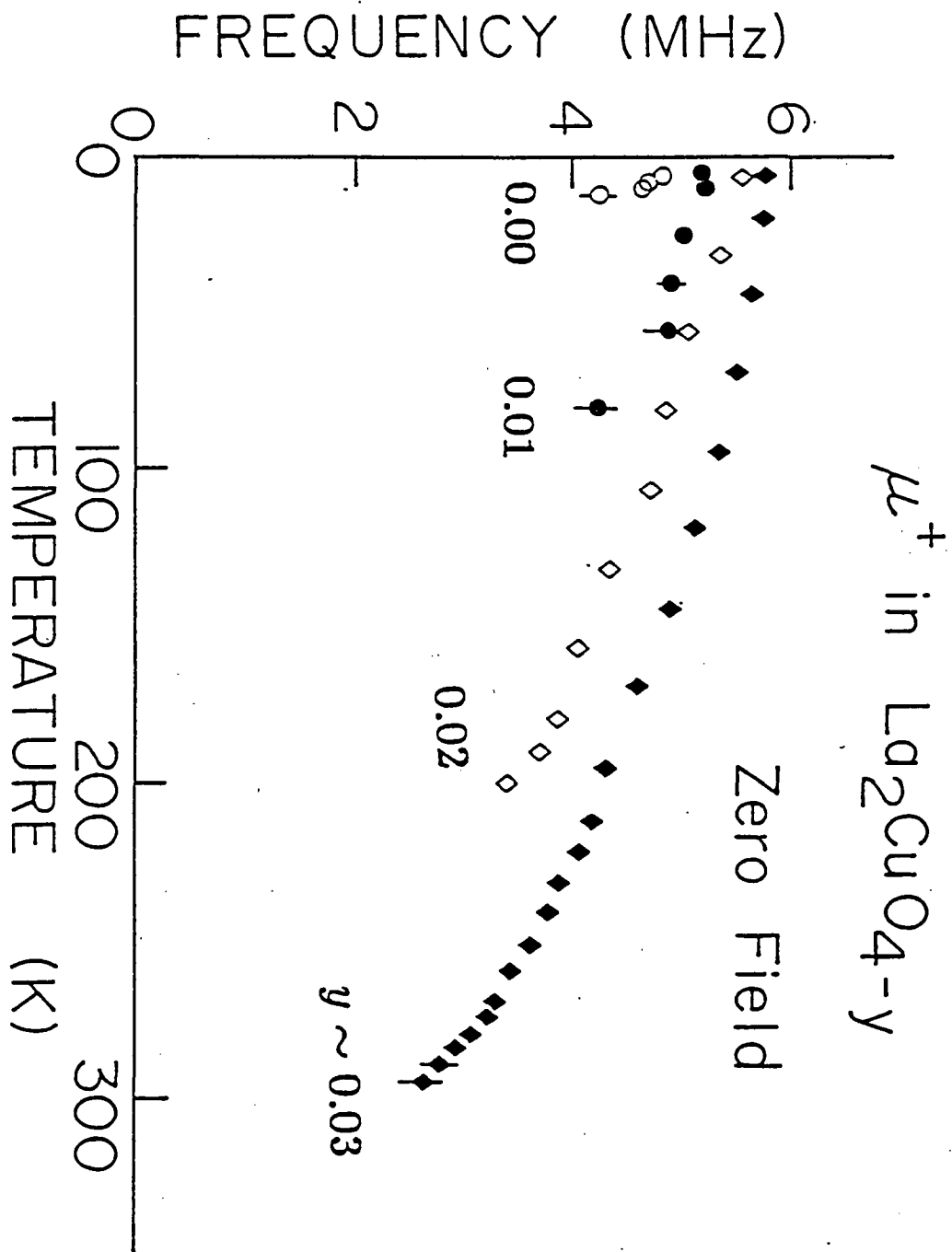


Figure 1.

La<sub>2</sub>CuO<sub>4-8</sub>

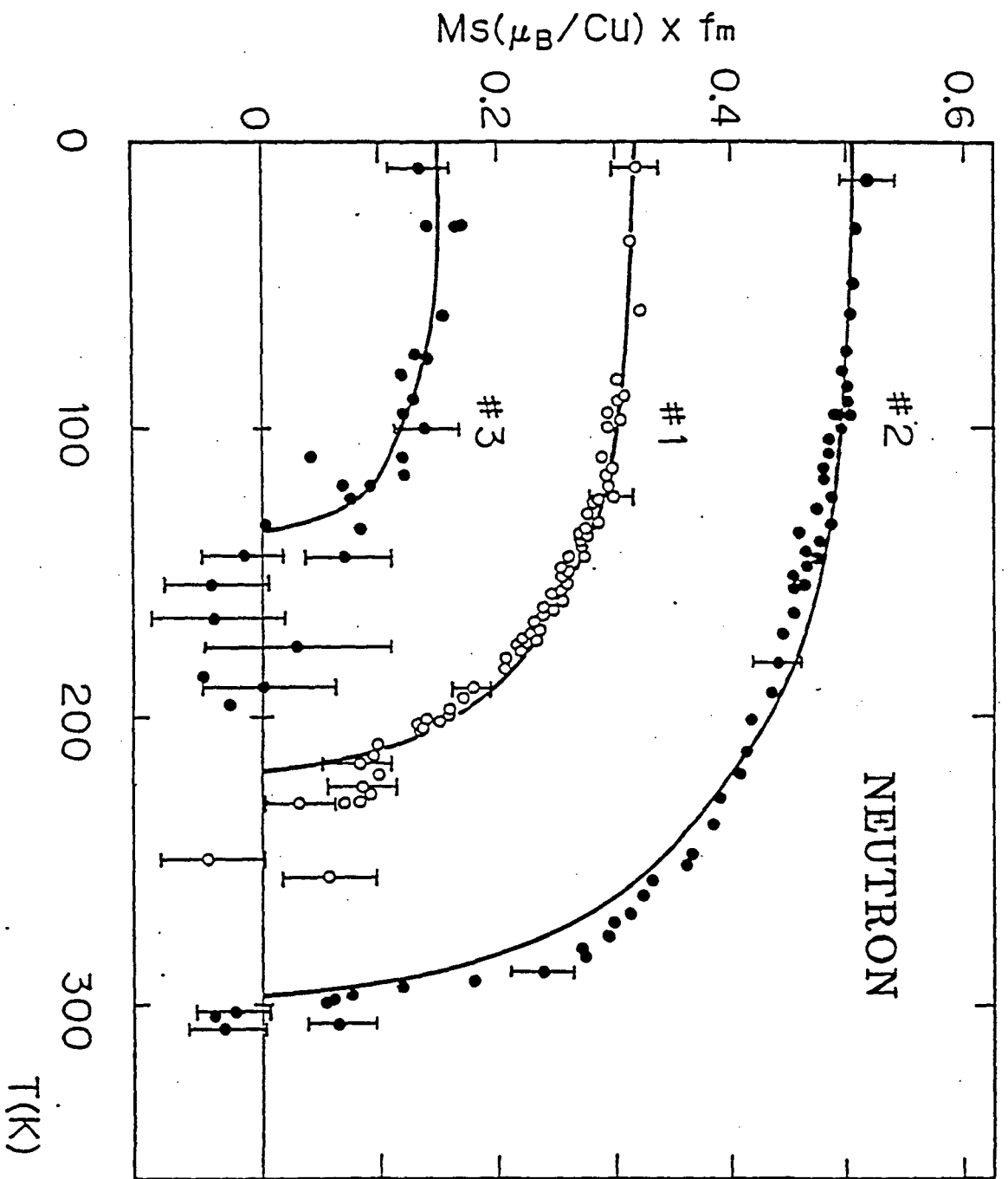
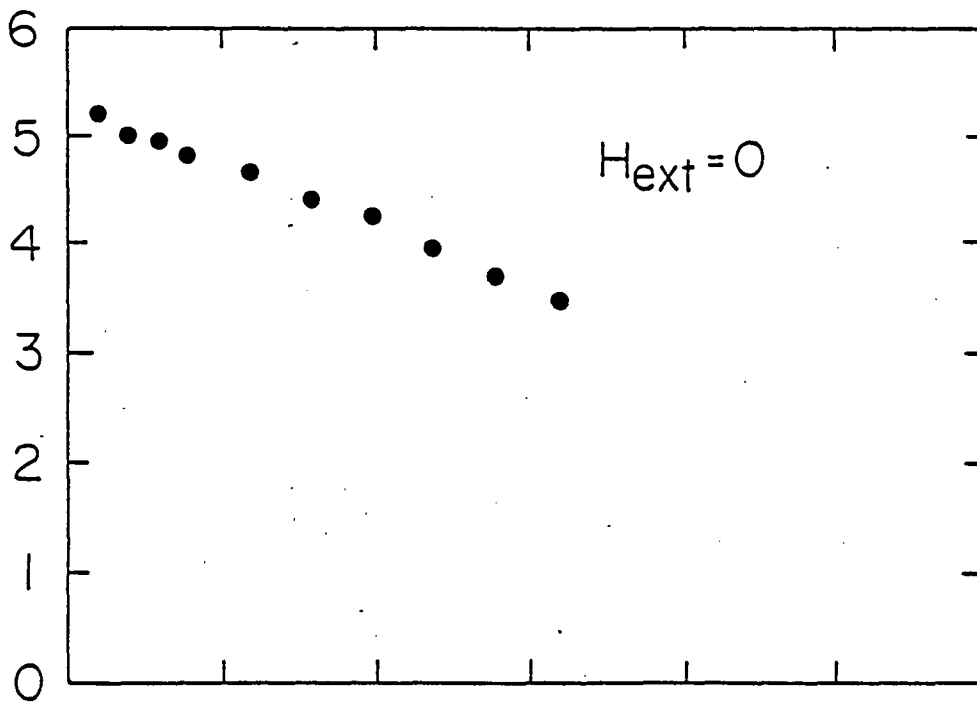


Figure 2.

$\mu^+$  in  $\text{La}_2\text{CuO}_4$  Single Crystal

MUON FREQUENCY (MHz)



PARAMAG FRACTION (%)

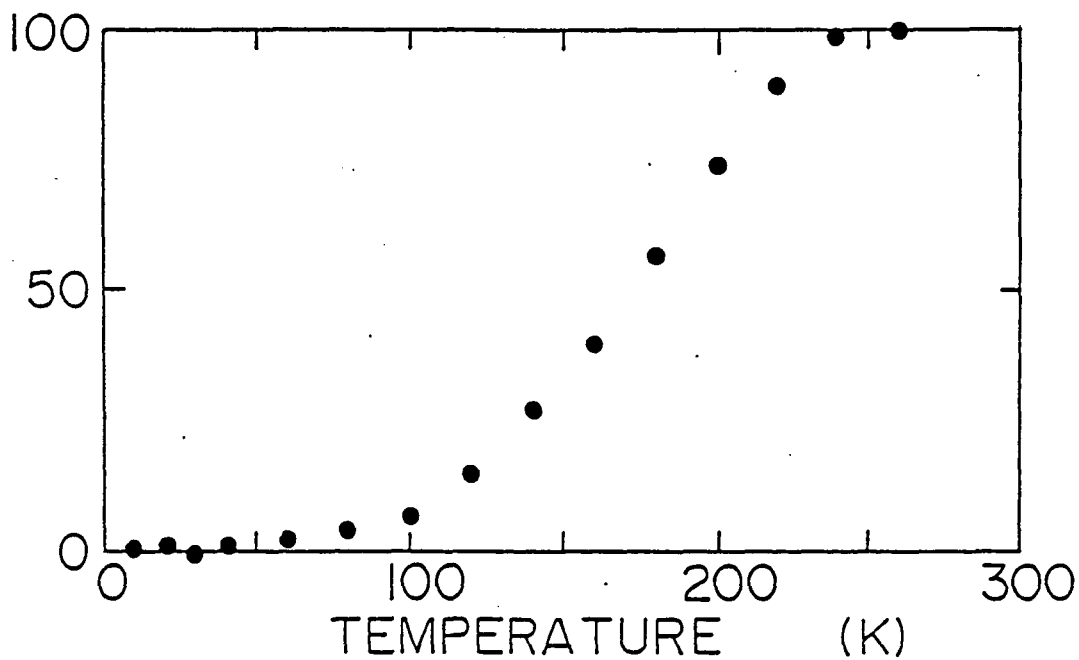


Figure 3.

APPENDIX E

## Coexisting Static Magnetic Ordering and Superconductivity

P-14

in  $CeCu_{2.1}Si_2$  Found by Muon Spin RelaxationY.J. Uemura<sup>1)</sup>, W.J. Kossler<sup>2)</sup>, X.H. Yu<sup>2)</sup>, H.E. Schone<sup>2)</sup>, J.R. Kempton<sup>2),a)</sup>C.E. Stronach<sup>3)</sup>, S. Barth<sup>4)</sup>, F.N. Gygax<sup>4)</sup>, B. Hitti<sup>4),2)</sup>, A. Schenck<sup>4)</sup> /C. Baines<sup>5)</sup>, W.F. Lankford<sup>6)</sup>, Y. Ōnuki<sup>7)</sup>, T. Komatsubara<sup>7)</sup>

- 1) *Brookhaven National Laboratory, Upton, New York 11979*
- 2) *Department of Physics, College of William and Mary, Williamsburg, Virginia 23185*
- 3) *Department of Physics, Virginia State University, Petersburg, Virginia 23808*
- 4) *Institute for Intermediate Energy Physics, ETH Zürich, c/o PSI (formerly SIN), CH-5294, Villigen, Switzerland*
- 5) *PSI (formerly SIN), CH-5294, Villigen, Switzerland*
- 6) *Physics Department, George Mason University, Fairfax, Virginia 22030*
- 7) *Institute of Materials Science, University of Tsukuba, Sakura-mura, Ibaraki 305, Japan*

(January, 1988)

## ABSTRACT

Zero- and longitudinal-field muon spin relaxation measurements on a heavy-fermion system  $CeCu_{2.1}Si_2$  have revealed an onset of static magnetic ordering below  $T_M \sim 0.8K$ , which coexists with superconductivity below  $T_C = 0.7K$ . The line shapes of the observed muon spin depolarization functions suggest an ordering in either spin glass or incommensurate spin-density-wave state, with a small averaged static moment of the order of  $0.1\mu_B$  per formula unit at  $T \rightarrow 0$ . (PACS Nos. 75.20.H, 76.75, 74.70.H)

$CeCu_2Si_2$  belongs to a group of Cerium or Uranium intermetallic compounds, called heavy-fermion systems<sup>1</sup>, which are characterized by the extremely large  $T$ -linear term  $C = \gamma T$  with  $\gamma \sim 1 \text{ Joule/mole deg}^2$  of the electronic specific heat  $C$  at low temperatures inferring very large effective mass  $m^*$ . In 1979, Steglich *et al.*<sup>2</sup> found a superconducting transition in  $CeCu_2Si_2$  at  $T \sim 0.5K$ , as the first example of the superconducting ground state of a heavy-fermion system. This discovery triggered extensive study of superconductivity and its possible relation with magnetism in the highly correlated heavy electron systems<sup>1,3</sup>. Although there are some susceptibility measurements<sup>4,5</sup> which suggest magnetic ordering of non-superconducting systems  $Ce_{1-y}La_yCu_2Si_2$  with  $y \geq 0.2$  (ref. 5) and  $CeCu_xSi_2$  with  $x = 1.9$  (ref. 4), so far it has been common to assume<sup>1</sup> a purely superconducting ground state without magnetic ordering for the superconducting compounds  $CeCu_xSi_2$  with  $2.0 \leq x \leq 2.2$  (ref. 6). In this paper, we present the first direct evidence from zero-field muon spin relaxation measurements that superconductivity and static magnetic ordering coexist in  $CeCu_{2.1}Si_2$ . Muon Spin Relaxation ( $\mu SR$ )<sup>7</sup> is a very powerful tool to detect static magnetic ordering<sup>8,9</sup>. Previous applications of  $\mu SR$  to heavy-fermion systems led to discoveries of magnetic ordering with quite small ordered moments ( $0.001 \sim 0.05 \mu_B$ ) in superconducting  $UPt_3$  (ref. 10) and non-superconducting  $CeAl_3$  (ref. 11). With the present results on  $CeCu_{2.1}Si_2$ , we now have three heavy-fermion superconductors,  $CeCu_{2.1}Si_2$ ,  $UPt_3$ , and  $URu_2Si_2$  (ref. 12), which show co-existing magnetic orderings.

Superconductivity of the stoichiometric  $CeCu_{2.0}Si_2$  is known to be somewhat unstable<sup>5</sup>. A small amount of additional  $Cu$  helps to stabilize the superconductivity of  $CeCu_xSi_2$  with  $x = 2.1 \sim 2.2$  whose superconducting transition temperature  $T_C$  is around 0.7 K

(ref. 6). We therefore prepared a poly-crystalline sample of  $CeCu_{2.1}Si_2$  by the method described in ref. 6. Figure 1 shows resistivity measured on a piece cut off from the sample of  $CeCu_{2.1}Si_2$  used in the present  $\mu$ SR measurement. Reference 6 describes detailed resistivity and specific-heat measurements on a few poly-crystalline samples of  $CeCu_xSi_2$  with  $x = 1.9 \sim 2.2$  made with the same method. The present specimen has  $T_C$  at around  $0.7 K$ , and the temperature dependence of resistivity shows the same curvature as reported in ref. 6. To further characterize the present sample, we made a neutron scattering measurement of the crystal structure, and confirmed that it is a single phase material without any minor phase within the experimental accuracy of a few volume percent.

We started zero-field  $\mu$ SR measurements on the present sample of  $CeCu_{2.1}Si_2$  at the AGS muon channel of Brookhaven National Laboratory by using a  $^3He$ -cryostat. A rapid increase of the muon spin relaxation rate was found with decreasing temperature below  $T \sim 0.8K$ . We then continued the measurement at SIN, Switzerland, by using a surface muon beam and a dilution refrigerator. The facility at SIN allowed full access to a wide temperature region with high-statistics data as we report in this paper. A positive muon beam was stopped at the sample of  $CeCu_{2.1}Si_2$  ( $2cm \times 1cm \times 0.5cm$ ) mounted on a cold finger of the dilution cryostat, and the muon-decay positrons were recorded mainly with a counter placed in the forward direction with respect to the beam direction. The counting rate  $I(t)$  of this counter is given as

$$I(t) \propto \exp(-t/\tau_\mu)[1 - AG_z(t)], \quad (1)$$

where  $\tau_\mu$  is the muon lifetime  $2.2 \mu sec$ ,  $A$  is the initial decay asymmetry ( $A \sim 0.25$  at the present condition), and the relaxation function  $G_z(t)$  represents the time evolution of muon spin polarization.

Figure 2-(a) shows the relaxation function  $G_z(t)$  thus observed in zero field. The relaxation rate increased rapidly below  $T \sim 0.8K$  with decreasing temperature. In general, the depolarization of muon spins in zero field can be due either to randomness of the static internal local field  $H_{int}$  or to the fluctuating dynamic local fields. One can distinguish between these two cases by making measurements in the longitudinal external magnetic field  $H_{ext}$  applied parallel to the initial muon spin direction (i.e., the direction of muon beam, denoted as  $z$  direction hereafter). When the internal field is static and  $H_{ext}$  is larger than  $H_{int}$ ,  $H_{ext}$  can align the local field  $\vec{H}_{loc} = \vec{H}_{int} + \vec{H}_{ext}$  to be nearly parallel to the muon spin polarization, thus keeping  $G_z(t)$  finite. In contrast, the dynamic spin fluctuations are usually much faster than the corresponding Zeeman frequency  $\omega = \gamma_\mu H_{ext}$  ( $\gamma_\mu = 2\pi \times 13.554 MHz/kG$ ) of  $\mu^+$ , so that there is almost no effect of  $H_{ext}$  on  $G_z(t)$  for the dynamic case. We have performed such measurements in  $H_{ext} = 250G$  and  $1kG$  at  $T = 0.1K$  as shown in Fig. 2-(b). The longitudinal fields suppress the depolarization and change  $G_z(t)$  remarkably. This indicates that the depolarization observed in zero field is due mainly to the static random local fields of the order of  $100 \sim 200G$ . Similar measurements with  $H_{ext}$  confirmed that the depolarization at  $T = 0.8K$  is also due to the static fields.

The line shapes of  $G_z(t)$  in zero field shown in Fig. 2-(a) resemble those observed in the dilute-alloy spin glasses  $CuMn$  or  $AuFe$  (ref. 8). The lack of coherent oscillation indicates that the magnitude of the static internal field  $|H_{int}|$  has a wide distribution. For a uniform  $|H_{int}|$ , one should have seen a muon spin precession as reported in refs. 9 and 11.  $G_z(t)$  in Fig. 2-(a) at  $T = 0.05K$  starts with a Gaussian-like shape at  $t \rightarrow 0$ . This is somewhat different from the case in the dilute-alloy spin glasses where  $G_z(t \rightarrow 0)$  decays

with an exponential-like shape when the temperature is well below the susceptibility-cusp temperature  $T_g$ . In this paper, we do not develop a complicated theory to account for this line shape, but rather adopt a phenomenological relaxation function

$$G_z(t) = \frac{A_1}{A} \exp(-\frac{1}{2}\sigma^2 t^2) + \frac{A_2}{A} \exp(-\Delta t) \quad (2)$$

to fit the observed data. The first term corresponds to the quick initial decay caused by the  $x$ - and  $y$ - components of the static random local fields. The second term represents the tail arising from the component of  $H_{int}$  parallel to the initial muon spin direction (i.e., the  $z$ -direction). Reasonably good fits to the data at all different temperatures  $0.05K \leq T \leq 1.0K$  were obtained when we assumed  $A_1/A \cong 2/3$ ,  $A_2/A \cong 1/3$ , with  $A = 0.25$ . The present counter configuration without the backward counter, however, made it difficult to determine the second term of eq. (2) accurately. Therefore, the decay rate  $\Delta$  of the tail, ranging around  $\Delta \sim 1.0\mu\text{sec}^{-1}$ , may be subject to a large systematic error. In contrast, the first term of eq. (2) can be determined with reasonable precision. From the fit to eq. (2) represented by the solid lines in Fig. 2-(a), we thus obtained the muon spin relaxation rate  $\sigma$  as shown in Fig. 3.

The relaxation rate  $\sigma$  in Fig. 3 increases rapidly with decreasing temperature below  $T \sim 0.8K$ . This indicates the onset of a random but static magnetic order at the magnetic ordering temperature  $T_M \sim 0.8K$ . Because of the limited accuracy of the temperature measurements and control with the cold-finger cryostat, as represented by the horizontal error-bars in Fig. 3, we can not identify whether the magnetic and superconducting orderings occur simultaneously or whether  $T_M$  and  $T_C$  are somewhat different. It is evident from Figs. 1-3, however, that the superconductivity and magnetic ordering coexist below

$T \sim 0.7K$  in  $CeCu_{2.1}Si_2$ . The present results indicate that more than 90 volume percent of the specimen undergoes the magnetic ordering. The relaxation rate  $\sigma$  in Fig. 3 represents a measure of the width of the static internal fields as  $\sigma \sim \gamma_{\mu} \sqrt{\langle (\Delta H_{int})^2 \rangle}$ . The observed value of  $\sigma \sim 10\mu sec^{-1}$  at  $T \rightarrow 0$  corresponds to the static random local fields of the order of  $\sigma/\gamma_{\mu} \sim 120G$ . In most magnetic materials, local fields at muon sites are due mainly to the dipolar field from the surrounding moments. Since  $\mu^+$  is a point-like probe in real space, and since information on the muon stopping site is lacking, it is not easy to accurately estimate the spatial spin structure of the magnetically ordered state of  $CeCu_{2.1}Si_2$ . It is, however, possible to note the following.

Spin glass ordering is one of the most likely spin structures which produce a large distribution of  $H_{int}$  as observed in the present experiment (see ref. 8). This picture is consistent with the observation of a strong effect of external fields on the susceptibility measurements of  $CeCu_{1.9}Si_2$  (ref. 4). If one assumes that the majority of  $Ce$  (or  $Cu$ ) atoms participate in the magnetic ordering, the observed width  $\sim 120G$  of  $H_{int}$  corresponds to the dipolar field from the ordered moment of the order of  $0.1 \mu_B$ . If instead the small population of  $Ce^{3+}$  ions forms a spin glass with an ordered moment of  $5\mu_B$ , like dilute-alloy spin glasses, then the observed value of  $\sigma$  corresponds to an ordering of about a few percent of the  $Ce$  atoms. The latter picture is advocated in ref. 4 for the case of  $CeCu_{1.9}Si_2$ . The Gaussian-like decay of  $G_z(t \rightarrow 0)$  may favor the former type of spin glass, but then one faces the difficult question as to the origin of the frustration of the exchange interactions. An incommensurate spin-density-wave state, like that observed in  $CePb_3$  (ref. 13), is another possible spin structure which gives the local field at the muon

site a wide distribution. Unfortunately, the present experiment alone can not distinguish the above mentioned three possible spin structures.

A neutron scattering experiment on  $CeCu_{2.1}Si_2$  is underway<sup>14</sup> to study spatial spin correlation. For such a small averaged moment as  $\sim 0.1\mu_B$ , however, the magnetic scattering intensity of neutrons is very small. Neutron measurements become even more difficult when the spin glass ordering makes the scattering diffusive in reciprocal space. In this respect, the present experiment demonstrates the unique capability of zero-field  $\mu$ SR to detect magnetic orderings with small averaged moments. In the previous  $\mu$ SR study on the same specimen of  $CeCu_{2.1}Si_2$  performed in the transverse external magnetic field<sup>15</sup>, the depolarization of muon spins observed below  $T \sim 0.8K$  was tentatively attributed to the inhomogeneous penetration of the transverse external field in the type-II superconducting state. Zero-field  $\mu$ SR can detect the magnetic ordering without the complication of the field penetration. The present results indicate that a major part of the depolarization observed in the transverse field was due to the static magnetic ordering. In order to find out whether the superconductivity and magnetic ordering occur at the same temperature or at different temperatures, we are planning to perform additional  $\mu$ SR measurements on specimens with different  $Cu$  stoichiometry which may have different  $T_M$  (see ref. 4).

Recently, a heavy-fermion superconductor  $UPt_3$  ( $T_C \sim 0.5K$ ) was found<sup>10</sup> to order magnetically below  $T \sim 5K$  with an extremely small averaged moment of  $\sim 0.001\mu_B$ .  $URu_2Si_2$  is another superconducting heavy-fermion system ( $T_C \sim 1.0K$ ) which orders antiferromagnetically below  $T_N \sim 17K$  with an ordered moment of  $0.03\mu_B$  per Uranium atom<sup>12</sup>.  $UBe_{13}$  is so far the only remaining heavy-fermion superconductor without an

identified magnetic ground state, yet there is a report<sup>16</sup> which suggests a possible antiferromagnetic ordering in  $UBe_{13}$  doped with a small amount of  $Th$ . Together with the present results on  $CeCu_{2.1}Si_2$ , these features indicate that the magnetic ordering with extremely small averaged moment may be a common feature of heavy-fermion superconductors.

In summary, zero-field  $\mu$ SR measurements on  $CeCu_{2.1}Si_2$  have shown clear evidence of static magnetic ordering below  $T_M \sim 0.8K$  with a very small averaged moment of  $\sim 0.1\mu_B$  in either a spin glass or an incommensurate spin-density-wavestate. This ordering coexists with superconductivity below  $T_C = 0.7K$ . Further experimental and theoretical studies are clearly needed for the full understanding of the role of such magnetic orderings on the superconductivity of heavy-fermion systems.

We would like to acknowledge useful discussions with P.B. Allen, K. Kakurai, M. Steiner and E. Recknagel. We thank W. Schönig for help on the measurements at Brookhaven. This work is supported by the Division of Materials Sciences, US Department of Energy under contract 76-AC02-CH00016, the National Science Foundation under DMR 8503223 and INT 8413978, NASA under NAG-1-416, and by the Japanese Ministry of Education, Science and Culture under the Grant-In-Aid for Scientific Research.

## REFERENCES

- a) present address: TRIUMF, UBC, Vancouver, B.C., V6T 2A3, Canada.
1. for a review of heavy-fermion systems, see, for example, G.R. Stewart, *Rev. Mod. Phys.* 56, 755 (1984).
  2. F. Steglich *et al.*, *Phys. Rev. Lett.* 43, 1892 (1979).
  3. see, for example, papers presented in the sessions of heavy-fermion systems in recent conferences, in *J. Magn. Magn. Matr.* 31 – 34 (1983); 47 – 48 (1985); 54 – 57 (1986); 63 – 64 (1987); and *J. Appl. Phys.* 55 (1984); 57 (1985); 61 (1987).
  4. U. Rauchschwalbe *et al.*, *J. Magn. Magn. Matr.* 47 – 48, 33 (1985).
  5. F.G. Aliev *et al.*, *J. Low Temp. Phys.* 57, 61 (1984); N.B. Brandt and V.V. Moshchalkov, *Adv. Phys.* 33, 373 (1984).
  6. Y. Ōnuki *et al.*, *J. Phys. Soc. Japan* 56, 1454 (1987).
  7. for general aspects of muon spin relaxation, see proceedings of four previous international conferences, *Hyperfine Interact.* 6 (1979); 8 (1981); 17 – 19 (1984); 31 (1986).
  8. Y.J. Uemura *et al.*, *Phys. Rev. B* 31, 546 (1985).
  9. Y.J. Uemura *et al.*, *Phys. Rev. Lett.* 59, 1045 (1987).
  10. D.W. Cooke *et al.*, *Hyperfine Interact.* 31, 425 (1986).
  11. S. Barth *et al.*, *Phys. Rev. Lett.* 59, 2991 (1987).
  12. T.T.M. Palstra *et al.*, *Phys. Rev. Lett.* 55, 2727 (1985); M.B. Maple *et al.*, *ibid.* 56, 185 (1986); C. Broholm *et al.*, *ibid.* 58, 1467 (1987).
  13. C. Vettier *et al.*, *Phys. Rev. Lett.* 56, 1980 (1986).

14. Y.J. Uemura *et al.*, unpublished.
15. Y.J. Uemura *et al.*, *Hyperfine Interact.* 31, 413 (1986).
16. B. Batlogg *et al.*, *Phys. Rev. Lett.* 55, 1319 (1985).

## FIGURE CAPTIONS

Fig. 1. Resistivity measured on a piece of  $CeCu_{2.1}Si_2$  cut off from the present specimen used in the  $\mu$ SR measurements. Superconducting transition occurs at  $T_C = 0.7K$ .

Fig. 2. (a) Muon spin relaxation function  $G_z(t)$  in zero field observed in  $CeCu_{2.1}Si_2$ . Solid lines represent fits to eq. (2). (b) Muon spin relaxation function in  $CeCu_{2.1}Si_2$  observed at  $T = 0.1K$  in longitudinal external magnetic fields LF of 0G, 250G, and 1kG. Solid lines are guides to the eye.

Fig. 3. Muon spin depolarization rate  $\sigma$ , as defined in eq. (2), derived from the relaxation functions observed in  $CeCu_{2.1}Si_2$  in zero field. The onset of magnetic ordering is seen around  $T_M \sim 0.8K$ .

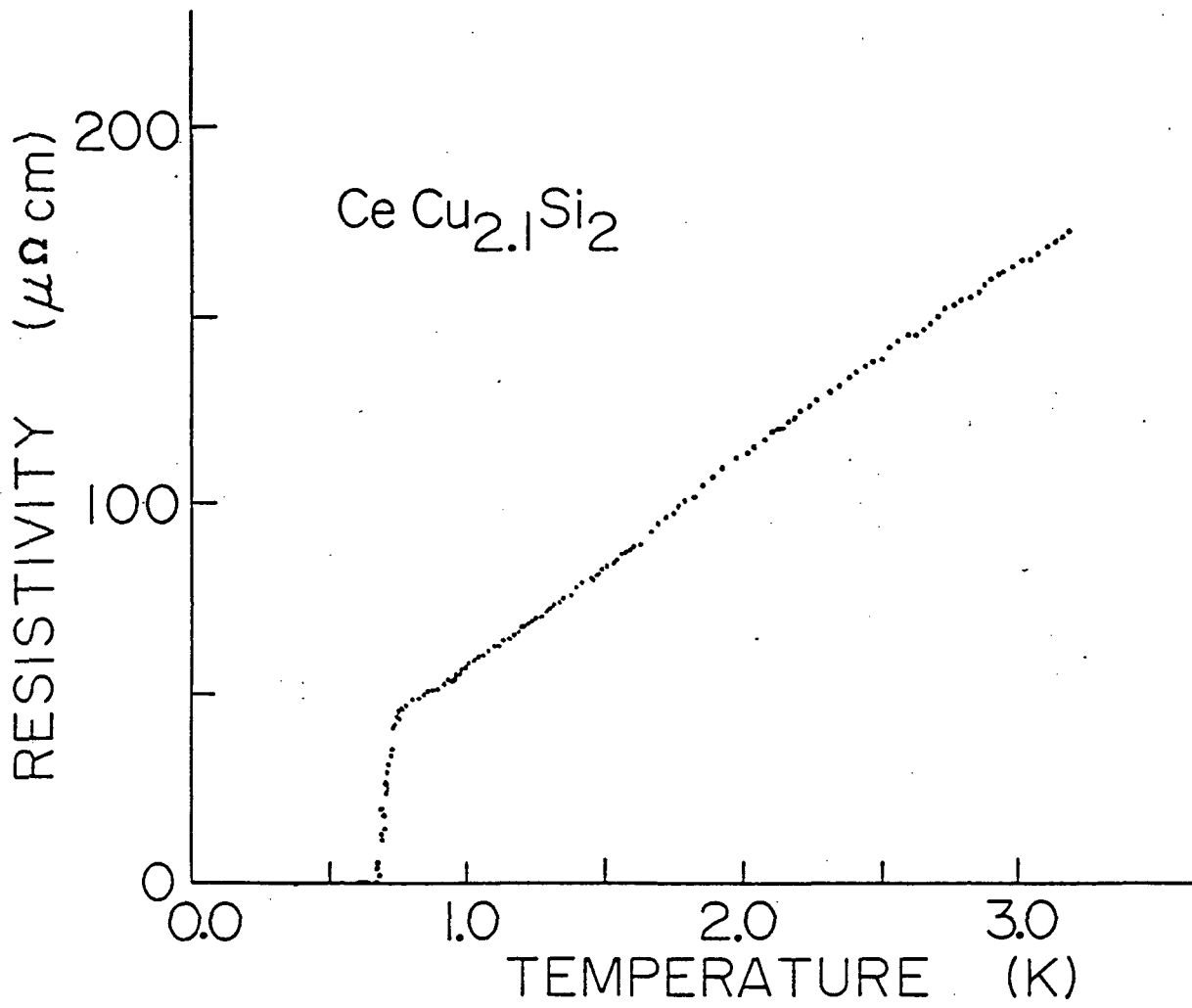


Figure 1

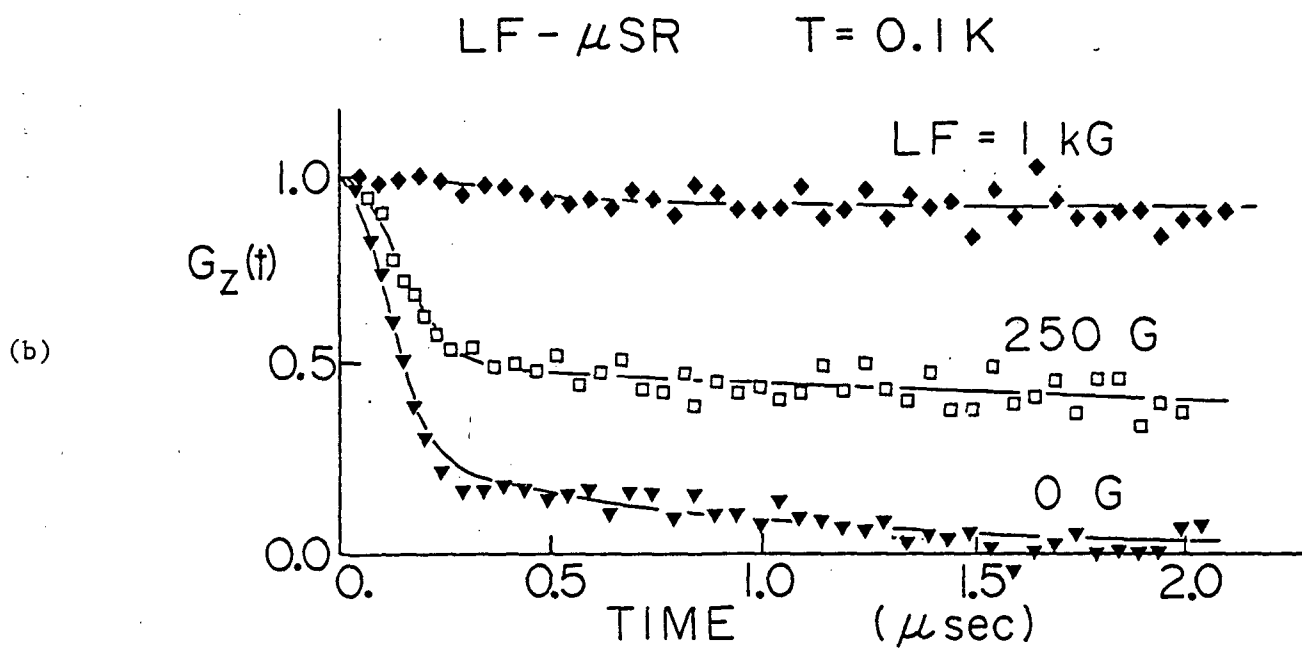
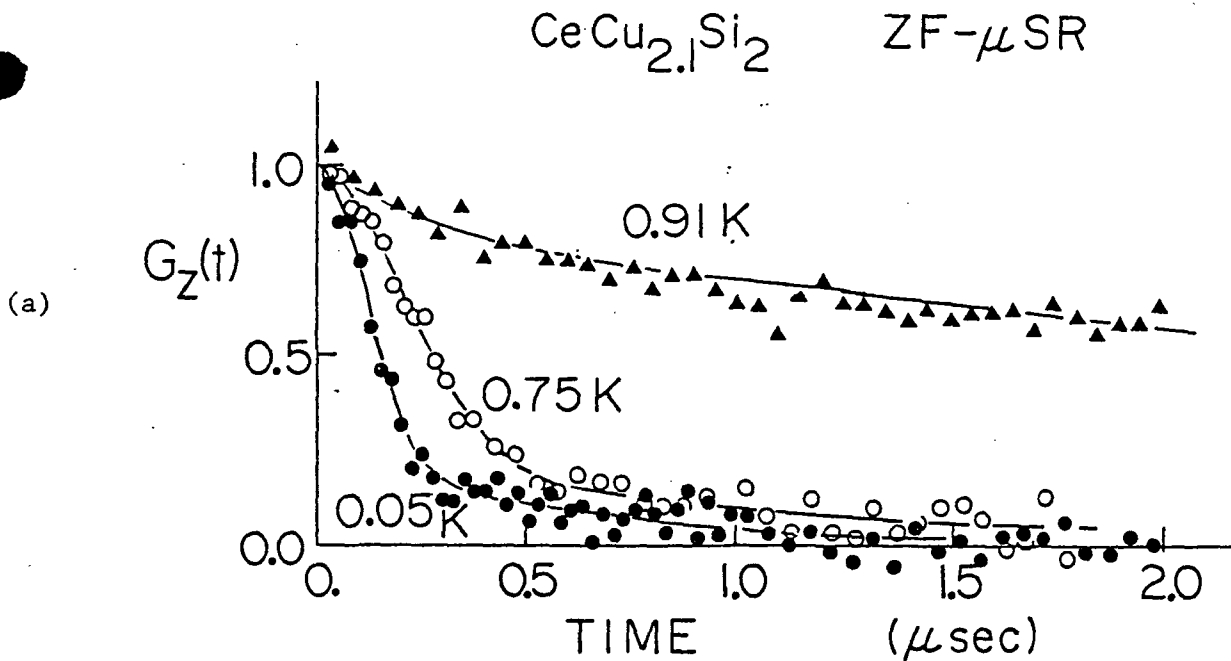


Figure 2

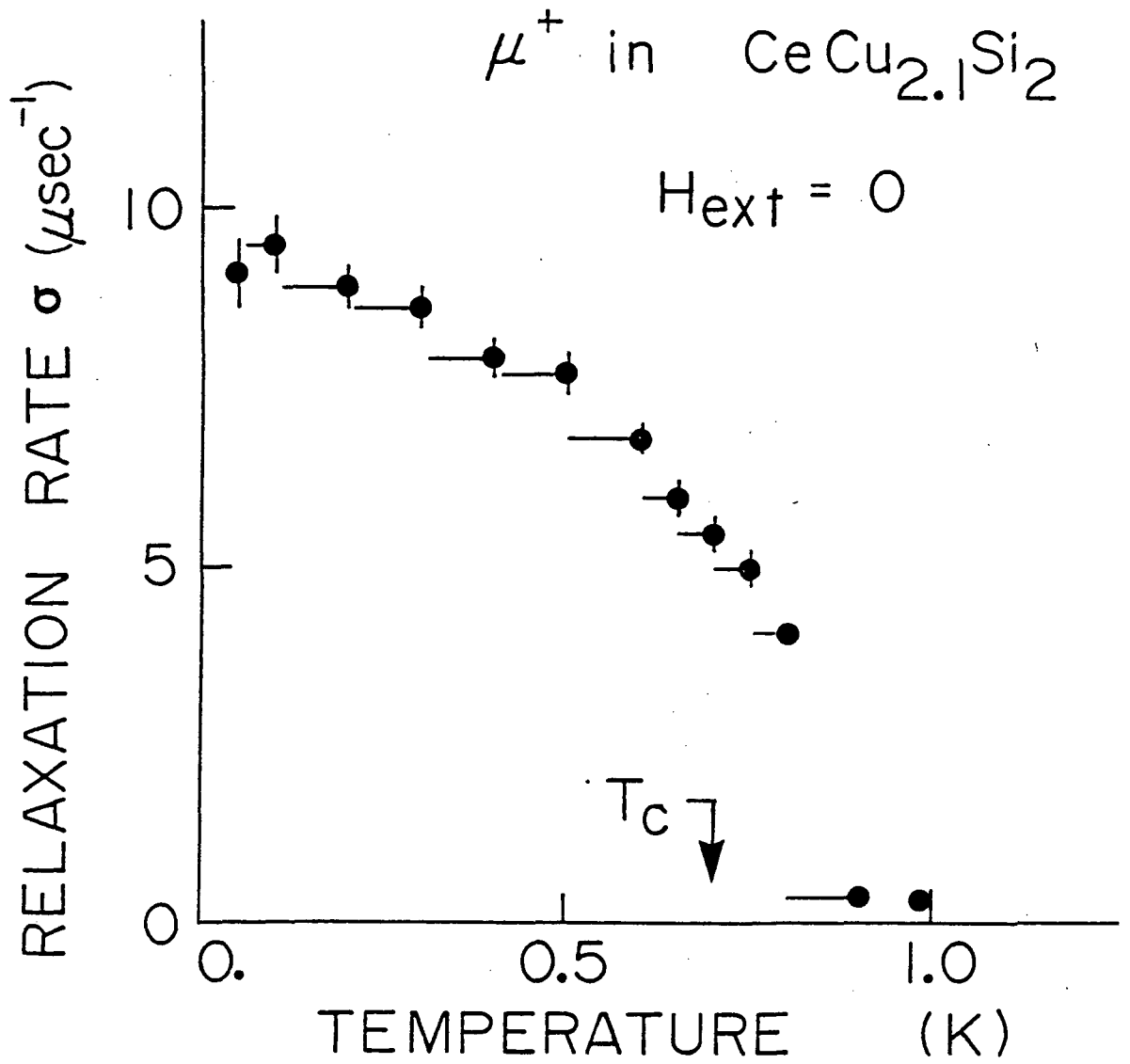


Figure 3

APPENDIX F

Static Magnetic Ordering of  $CeCu_{2.1}Si_2$ 

## Found by Muon Spin Relaxation

Y.J. Uemura<sup>1)</sup>, W.J. Kossler<sup>2)</sup>, X.H. Yu<sup>2)</sup>, H.E. Schone<sup>2)</sup>, J.R. Kempton<sup>2),a)</sup>C.E. Stronach<sup>3)</sup>, S. Barth<sup>4)</sup>, F.N. Gygax<sup>4)</sup>, B. Hitti<sup>4),2)</sup>, A. Schenck<sup>4)</sup> /C. Baines<sup>5)</sup>, W.F. Lankford<sup>6)</sup>, Y. Ōnuki<sup>7)</sup>, T. Komatsubara<sup>7)</sup>

- 1) *Brookhaven National Laboratory, Upton, New York 11973*
- 2) *Department of Physics, College of William and Mary, Williamsburg, Virginia 23185*
- 3) *Department of Physics, Virginia State University, Petersburg, Virginia 23803*
- 4) *Institute for Intermediate Energy Physics, ETH Zürich, c/o PSI (formerly SIN), CH-5294, Villigen, Switzerland*
- 5) *PSI (formerly SIN), CH-5294, Villigen, Switzerland*
- 6) *Physics Department, George Mason University, Fairfax, Virginia 22030*
- 7) *Institute of Materials Science, University of Tsukuba, Sakura-mura, Ibaraki 305, Japan*

*(submitted to the Interlaken HTSC-M<sup>2</sup>S meeting, February, 1988)*

## ABSTRACT

Zero- and longitudinal-field muon spin relaxation measurements on a poly-crystal sample of a heavy-fermion superconductor  $CeCu_{2.1}Si_2$  ( $T_C = 0.7K$ ) have revealed an onset of static magnetic ordering below  $T \sim 0.8K$ . The line shapes of the observed spectra in zero field indicate a wide distribution of static random local fields at muon sites, suggesting that the ordering is either spin glass or incommensurate spin-density-wave state. The observed width of the random local field at  $T = 0.05K$  corresponds to a small averaged static moment of the order of  $0.1\mu_B$  per formula unit.

$CeCu_2Si_2$  is the first heavy-fermion system which was found to become superconducting at  $T_C \sim 0.5K$  (ref. 1). Although there were signatures suggesting possible magnetic orderings in non-superconducting  $CeCu_{1.9}Si_2$  (ref. 2) and  $Ce_{1-y}La_yCu_2Si_2$  with  $y \geq 0.2$  (ref. 3), superconducting specimens  $CeCu_xSi_2$  with  $x = 2.0 \sim 2.2$  have so far been believed to have purely superconducting ground states without magnetic ordering. In this paper, we present direct evidence from muon spin relaxation ( $\mu$ SR) measurements that superconducting  $CeCu_{2.1}Si_2$  ( $T_C = 0.7K$ ) undergoes a random static magnetic ordering below  $T \sim 0.8K$ .

It is known that a small amount of off-stoichiometric excess  $Cu$  helps to stabilize the superconductivity of  $CeCu_2Si_2$ . Therefore, we prepared a polycrystal specimen of  $CeCu_{2.1}Si_2$  with the method described in ref. 4. The superconducting transition temperature  $T_C = 0.7K$  was determined by a resistivity measurement on a small piece cut out from the present specimen. A neutron scattering measurement on the crystal structure confirmed that there is no minor phase within the accuracy of a few volume percent.

Zero- and longitudinal-field  $\mu$ SR measurements were performed using polarized positive muon beams at AGS/BNL and SIN (Zürich) muon channels. In the zero-field measurements, very small depolarization of muon spins was observed above  $T = 0.9K$ , while the depolarization rate increased rapidly with decreasing temperature below  $0.8K$ . The zero-field muon spin relaxation functions  $G_z(t)$  (ref. 5) observed at different temperatures show no precession signal but have line shapes similar to those observed in dilute-alloy spin glasses<sup>5</sup>. This indicates that the magnitude of local fields at muon sites varies widely, in contrast to the cases for uniform ferro- or antiferromagnets.

A phenomenological form for the muon spin relaxation function

$$G_z(t) = \frac{A_1}{A} \exp(-\frac{1}{2}\sigma^2 t^2) + \frac{A_2}{A} \exp(-\Delta t), \quad (1)$$

with  $A_1/A \sim 2/3$  and  $A_2/A \sim 1/3$ , gives good fits to all the data observed in zero-field. The first (second) term of eq. (1) corresponds to the depolarization of muon spins by the components of internal fields perpendicular (parallel) to the initial polarization direction of the muon spins. Figure 1 shows the temperature dependence of the relaxation rate  $\sigma$ .

In order to distinguish whether this depolarization is due to static or fluctuating local fields, we have also performed  $\mu$ SR measurements by applying longitudinal external magnetic fields  $H_L = 250G$  and  $1kG$  parallel to the initial muon spin direction. The muon spin polarization had a finite value  $G_z(t) \sim 0.45$  with  $H_L = 250G$ , and  $G_z(t) \sim 0.95$  with  $H_L = 1kG$ , almost independent on time between  $0.5\mu\text{sec} \leq t \leq 2\mu\text{sec}$  at  $T = 0.1K$ . A similar decoupling of the random field was observed around  $T = 0.8K$ . These results indicate that the depolarization shown in Fig. 1 is due predominantly to the static random local fields. The rapid increase of  $\sigma$  below  $T \sim 0.8K$  then corresponds to the sharp onset of static magnetic ordering around the ordering temperature  $T_M = 0.8K$ . Due to the limited accuracy of the temperature measurements with the cold-finger dilution cryostat used in the present experiment, it is not clear whether the magnetic and superconducting orderings occur simultaneously at the same temperature or independently at different temperatures. It is, however, evident that the superconductivity and magnetic ordering coexist below  $T_C = 0.7K$ .

The wide distribution of the static random local fields, as observed in the present experiment, can be expected either for spin glass (SG) or incommensurate spin-density-

wave (ISDW) systems. The spin glass ordering is consistent with a large field dependence of the susceptibility observed in the non-superconducting system  $CeCu_{1.9}Si_2$  (ref.2). If one assumes that a majority of  $Ce$  (or  $Cu$ ) moments participate in the spin-glass freezing, the zero-field relaxation rate  $\sigma \sim 10\mu sec^{-1}$  (the width  $\sigma/\gamma\mu \sim 120G$  of the local field) observed at  $T = 0.05K$  corresponds to the dipolar field from a static moment of the order of 0.1 Bohr magneton per formula unit. If the small population of the  $Ce^{3+}$  ions with an ordered moment of  $5 \mu_B$  forms a spin glass, this value of  $\sigma$  is expected for the freezing moments on a few percent of the entire  $Ce$  atoms. From the present work alone, it is not possible to distinguish among the above-mentioned three possible spin structures (the two types of SG states and the ISDW state) of  $CeCu_{2.1}Si_2$  below  $T_M$ .

Recently, a heavy-fermion superconductor  $UPt_3$  ( $T_C \sim 0.5K$ ) was found<sup>10</sup> to order magnetically below  $T \sim 5K$  with an extremely small averaged moment of  $0.001 \sim 0.02\mu_B/U$  (refs 6,7).  $URu_2Si_2$  is another superconducting heavy-fermion system ( $T_C \sim 1.0K$ ) which orders antiferromagnetically below  $T_N \sim 17K$  with an ordered moment of  $0.03\mu_B$  per Uranium atom<sup>8</sup>. With the present results on  $CeCu_{2.1}Si_2$ , we now have three heavy-fermion superconductors which show coexisting magnetic ordering with extremely small ordered moments ( $0.001 \sim 0.1\mu_B$ ). This may then be a common feature of the superconductivity in heavy-fermion systems.

This work is supported by the Division of Materials Sciences, US Department of Energy under contract 76-AC02-CH00016, the National Science Foundation under DMR 8503223 and INT 8413978, NASA under NAG-1-416, and by the Japanese Ministry of Education, Science and Culture under the Grant-In-Aid for Scientific Research.

## REFERENCES

a) present address: TRIUMF, UBC, Vancouver, B.C., V6T 2A3, Canada.

1. F. Steglich *et al.*, Phys. Rev. Lett. 43, 1892 (1979).
2. U. Rauchschwalbe *et al.*, J. Magn. Magn. Matr. 47 - 48, 33 (1985).
3. F.G. Aliev *et al.*, J. Low Temp. Phys. 57, 61 (1984); N.B. Brandt and V.V. Moshchalkov, Adv. Phys. 33, 373 (1984).
4. Y. Ōnuki *et al.*, J. Phys. Soc. Japan 56, 1454 (1987).
5. Y.J. Uemura *et al.*, Phys. Rev. B31, 546 (1985).
6. D.W. Cooke *et al.*, Hyperfine Interact. 31, 425 (1986).
7. G. Aeppli *et al.*, Phys. Rev. Lett. 60, 615 (1988).
8. T.T.M. Palstra *et al.*, Phys. Rev. Lett. 55, 2727 (1985); M.B. Maple *et al.*, *ibid.* 56, 185 (1986); C. Broholm *et al.*, *ibid.* 58, 1467 (1987).

## FIGURE CAPTIONS

Fig. 1. Muon spin depolarization rate  $\sigma$ , as defined in eq. (1), derived from the relaxation functions observed in  $CeCu_{2.1}Si_2$  in zero field. The onset of magnetic ordering is seen around  $T_M \sim 0.8K$ . The superconducting transition temperature  $T_C$ , determined by a resistivity measurement on a piece cut off from the present specimen, is indicated by the arrow.

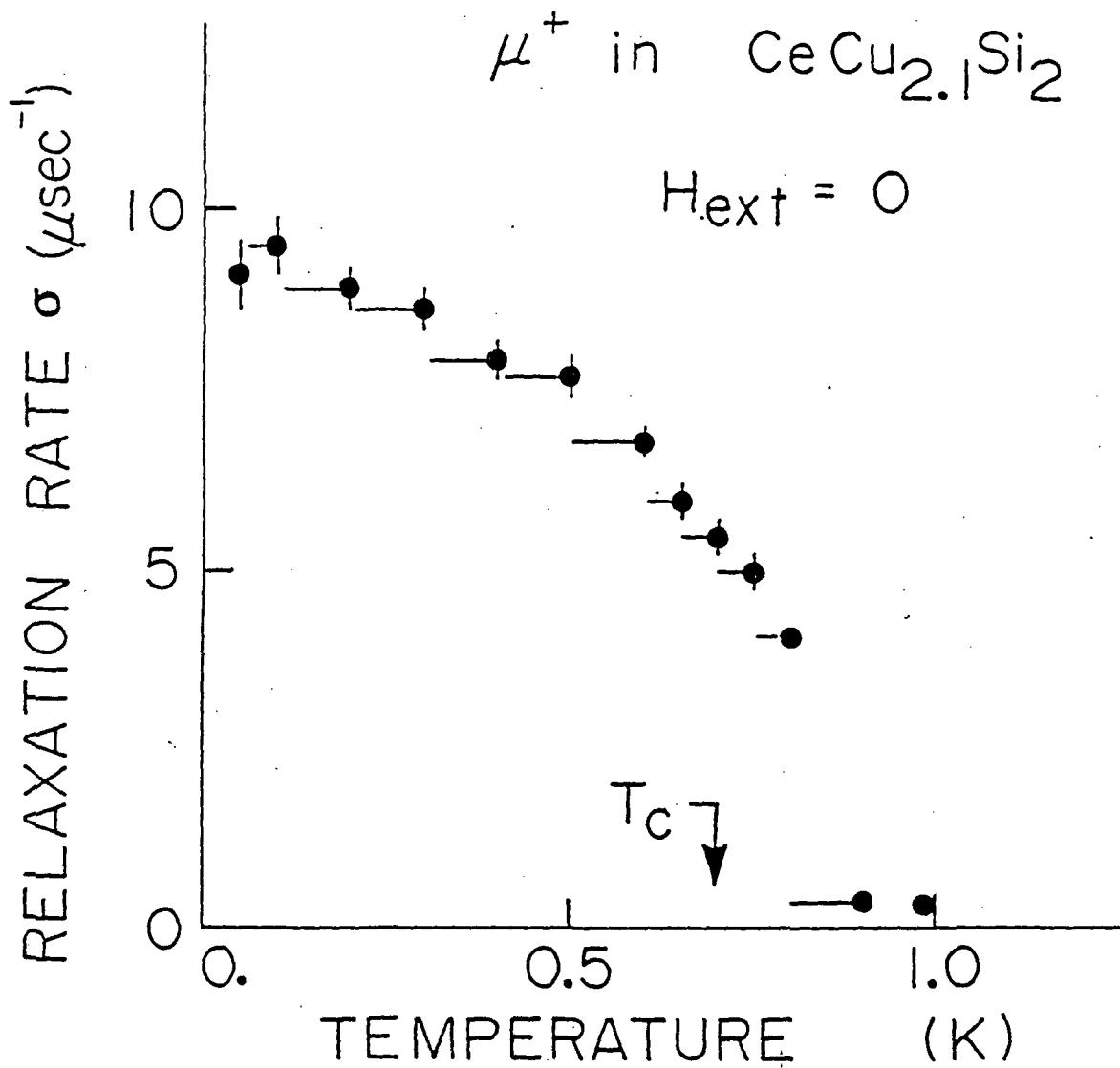


Figure 1.

APPENDIX G

## Muon Motion in Titanium Hydride

J. R. Kempton<sup>+</sup>, K. G. Petzinger, W. J. Kossler,  
H. E. Schone, and B. S. Hitti\*  
College of William and Mary, Williamsburg, Virginia 23185

C. E. Stronach and N. Adu  
Virginia State University, Petersburg, Virginia 23803

W. F. Lankford#  
George Mason University, Fairfax, Virginia 22030

J. J. Reilly  
Brookhaven National Laboratory, Upton, New York 11973

E. F. W. Seymour,  
University of Warwick, Coventry, England CV4 7AL

- + Current address: c/o TRIUMF, 4004 Wesbrook Mall, Vancouver, B. C., Canada V6T 2A3.
- \* Current address: Institut für Mittelenergiephysik, ETH Zürich, c/o SIN, CH-5234 Villigen, Switzerland.
- # Current address: Autonomous University of Nicaragua, Managua, Nicaragua.

Motional narrowing of the transverse-field muon spin rotation signal has been observed in  $\gamma$ -TiH<sub>x</sub> for x=1.83, 1.97, and 1.99. An analysis of the data for TiH<sub>1.99</sub> near room temperature indicates that the mechanism responsible for the motion of the muon out of the octahedral site is thermally activated diffusion with an attempt frequency comparable to the optical vibrations of the lattice. Monte Carlo calculations to simulate the effect of muon and proton motion upon the muon field-correlation time have been used to interpret the motional narrowing in TiH<sub>1.97</sub> near 500 K. The interpretation is dependent upon whether Bloembergen, Purcell, and Pound (BPP) theory or an independent spin-

pair relaxation model is used to obtain the vacancy jump rate from proton NMR  $T_1$  measurements. Use of BPP theory shows that the field-correlation time can be obtained if the rate of motion of the muon with respect to the rate of motion for the protons is decreased. An independent spin-pair relaxation model indicates that the field-correlation time can be obtained if the rate of motion for the nearest-neighbor protons is decreased.

## I. Introduction

This paper presents an interpretation of the motional narrowing of the  $\mu$ SR signal in  $\text{TiH}_x$  near room temperature for  $x = 1.99$  and near 500 K for  $x = 1.83$ . We report further analysis of the data of Kossler et al.<sup>1</sup>.

The high mobility of the hydrogen nuclei in metals has attracted the attention of scientists for over 100 years.<sup>2</sup> During the past 35 years, the technique of NMR has been used to determine the rate at which these hydrogen nuclei diffuse through metals and the mechanism responsible for this motion.<sup>3</sup> To accompany this, theorists have developed models for diffusion of light interstitials<sup>4</sup>. The development of these models has not only been helpful in the study of diffusion of hydrogen nuclei, but also other light particles such as the muon, which is often considered a light isotope of hydrogen ( $m_\mu \approx m_p/9$ ) due to similarities in charge and spin.

Fukai et al.<sup>5</sup> studied the isotopes of hydrogen in  $\alpha\text{-NbH}_x\text{D}_y$ . They found that the diffusion coefficient of protons decreased and that the proton activation energy approaches that of deuterons as more protons are replaced by deuterons. The muon extends markedly the range of masses studied. Up to now, the muon spin rotation ( $\mu$ SR) technique has been used to study  $\text{ZrH}_x$ <sup>6</sup>,  $\text{VH}_x$ <sup>6</sup>,  $\text{NbH}_x$ <sup>7</sup>,  $\text{NbD}_x$ <sup>7</sup>,  $\text{PdH}_x$ <sup>8</sup>,  $\text{TiH}_x$ <sup>1</sup>, and  $\text{YH}_x$ <sup>9</sup>. The results of experiments on FCC dihydride compounds ( $\text{TiH}_x$ ,  $\text{YH}_x$ , and  $\text{ZrH}_x$ ) exhibit the following characteristics: partial occupation of interstitial (octahedral) sites by the muon at low temperatures, escape from these sites and transfer to vacant substitutional (tetrahedral)

sites in the hydrogen sublattice as the temperature increases, and motional narrowing of the  $\mu$ SR frequency spectrum at higher temperatures due to motion of the protons, muons, or both. The results of studies on the other hydride compounds indicate that the muon occupies the vacant substitutional sites of the hydrogen sublattice upon entering the sample and that motional narrowing occurs as the temperature is increased, but it should be mentioned that the vacancy concentration in the hydrogen sublattice of these compounds was of the order of 30% or higher. Although there exist differences between the  $\mu$ SR studies of the various hydrogen-alloy systems, all of the compounds (except  $VH_{0.503}$ ) display an activation energy (as determined from the field-correlation time at the site of the muon) lower than that measured for the proton with NMR (Fig. 1). This is indeed surprising since one naively expects the motion of the muon to be impeded by that of the proton and that the measured activation would be equal to that of the proton.

In section 2 we present our analysis of the data<sup>1</sup> which yields a mean time of stay for a muon at an O site. In section 3, we develop and show the results of some Monte Carlo calculations of the field-correlation time for a muon at a substitutional site as a function of vacancy hopping rate. The results of these Monte Carlo simulations are compared to the  $TiH_{1.97}$  data ( $T \approx 500$  K) of Kossler et al.<sup>1</sup>.

## II. Activation of Muons Out of Octahedral Sites

The results of Kossler et al.<sup>1</sup> for  $\mu$ SR studies of  $\text{TiH}_x$  are shown in Fig. 2. They find that the muon depolarization rate,  $\Lambda$ , ( $G_x(t) = \exp(-\Lambda^2 t^2)$ ) in  $\text{TiH}_x$  for  $T < 200$  K can be parameterized by

$$\Lambda^2 = \Lambda_O^2(1-P) + P\Lambda_T^2 \quad (1)$$

where  $\Lambda_O$  and  $\Lambda_T$  are the depolarization rates for a muon in octahedral and tetrahedral sites, respectively,  $P$  is the probability of occupying a T site, and

$$P = 8(1 - x/2). \quad (2)$$

where  $x$  is the H/Ti ratio. The term inside the parenthesis is equal to the fractional vacancy concentration in the hydrogen sublattice and the factor of eight arises from assuming that the muon initially stops in an O site and jumps to one of eight nearest-neighbor T sites if vacant. The probability of a muon to occupy an O site is  $1-P$ , and thus these probabilities are 0.96, 0.88, 0.32 for  $x=1.99$ , 1.97, and 1.83, respectively. In order to understand the mechanism responsible for activation of the muon out of an octahedral site, let us turn our attention to the study of the  $\text{TiH}_{1.99}$  results since this system has the largest probability for a muon to occupy an O site.

The dip in the depolarization rate for  $\text{TiH}_{1.99}$  near room temperature is similar to that seen in niobium where the depression in  $\Lambda$  was due to muons activating out of relatively more

abundant shallow traps, and then finding deeper traps of lower concentration.<sup>10</sup> In niobium, the muons in the two traps have the same depolarization rate; whereas in TiH<sub>1.99</sub>, the muons in the abundant and shallow O-site traps have a larger depolarization rate than those in the sparser and deep T site traps, yielding an asymmetric dip in the depolarization rate.

The data for those temperature points (330 < T < 370 K) in the dip of the depolarization rate (Fig. 2) have been refit using a form (Abragamian) for the relaxation function which is better suited to motional narrowing than the Gaussian form.

$$G_X(t) = \exp[-\Delta^2 \tau_C^2 (\exp(-t/\tau_C) - 1 + t/\tau_C)] \quad (3)$$

where  $\Delta^2$  is the second moment of the field distribution and  $\tau_C$  is the field-correlation time. Any relaxation function (including the one above) can be represented as:  $G_X(t) = \exp[-\gamma(t)]$ , which allows the definition of an average muon spin decay rate,  $d\gamma/dt$ . When this rate is statistically weighted according to an exponential radioactive decay, we can define a dimensionless depolarization parameter:

$$\alpha = \int \exp(-t/\tau_\mu) (d\gamma/dt) dt, \quad (4)$$

where  $\tau_\mu$  is equal to the mean muon lifetime, 2.2  $\mu$ s. For the relaxation function listed in Eqn. 3,

$$\alpha = \Delta^2 \tau_\mu^2 \tau_C / (\tau_C + \tau_\mu). \quad (5)$$

' $\alpha$  of Eqn. 4 can be naturally related to many theoretical descriptions of depolarization. We have found that  $\alpha$  is not strongly dependent on the form chosen for  $\gamma(t)$ , and have used  $\gamma(t)$  from Eqn.3 for the purposes of obtaining  $\alpha$  through Eqn. 5. We used  $\alpha$  to obtain the mean time of stay at a particular site.

For  $\mu$ SR studies of Al(Cu), Kossler et al.<sup>11</sup> invoked a motional-narrowing theory for  $\gamma(t)$  to explain the diffusion and trapping of muons in terms of correlation functions:

$$\gamma(t) = \sum_i \Delta_i^2 \int_0^t dt' \int_0^{t'} dt'' F_i(t'') G_i(t'-t''). \quad (6)$$

where  $\Delta_i^2$ ,  $F_i(t)$  and  $G_i(t)$  are the second moment, probability of occupation and the autocorrelation function for a given site of type  $i$ , respectively. The summation extends over all interstitial site types, which for titanium hydride are the O and T sites. To define our model we proceed as follows:

- i) We assume that the muon initially stops randomly in octahedral sites and then proceeds immediately to a near neighbor tetrahedral site if one is vacant, so that the initial probability of occupying an octahedral site is equal to the probability that it would have no near neighbor vacant:  $(1-8c)$ , where  $c$  is the vacancy concentration.

- ii) Since the results reported by Kossler et al.<sup>1</sup> indicate that the muon does not activate out of a T site at room temperature, then

$$G_2(t) = 1. \quad (7)$$

The autocorrelation function for an O site (the shallow trap) is

$$G_1(t) = \exp(-t/\tau) \quad (8)$$

where  $\tau$  is a mean time of stay at an O site.

- iii) The transition rate  $r$  for a muon to migrate from O sites to a T site is  $8c/\tau$ , and there is no back migration to O sites. Thus  $F_O(t) = 8ce^{-rt}$  and  $F_T(t) = (1 - 8ce^{-rt})$ .

Using these assumptions, we can solve for the mean time of stay of the muon at an octahedral site as a function of  $\alpha$  by substituting Eqn. 6 into Eqn. 4

$$\begin{aligned} \tau = & 8c\tau_\mu [-0.5(1 + 8c + (1-8c)\Delta_2^2\tau_\mu^2/(\alpha - \Delta_2^2\tau_\mu^2)) + \\ & \pm [0.25\{(1 - 8c)\alpha/(\alpha - \Delta_2^2\tau_\mu^2)\}^2 + \\ & (1 - 8c)8c\Delta_1^2\tau_\mu^2/(\alpha - \Delta_2^2\tau_\mu^2)]^{1/2}]^{-1} \end{aligned} \quad (9)$$

and using the experimental  $\alpha$  calculated from Eqn. 5. The  $\pm$  arises because the same  $\alpha$  will occur for either slow O - O hops and weak migration to T sites, or for more rapid hops and greater migration.

We have used the fact that  $\alpha(T)$  is single valued at its experimental minimum and theoretically when the  $\pm$  bracket is zero to determine the effective vacancy concentration,  $c$ . Upon substituting in  $0.059(3) \mu\text{s}^{-1}$ ,  $0.127(3) \mu\text{s}^{-1}$ ,  $0.185(3) \mu\text{s}$  and  $2.2 \mu\text{s}$  for  $\Delta_2^2$ ,  $\Delta_1^2$ ,  $\alpha$  and  $\tau_\mu$ , we find  $c$  to be  $0.015(6)$  which corresponds to  $x=1.97(1)$  and agrees with the known concentration of  $1.99(2)$ .

Using the calculated value for the effective vacancy concentration, we calculated  $\tau_s(T)$  and show it in Fig. 3. The line is a least squares fit to an Arrhenius form,

$$\tau = \tau_0 \exp(E_a/kT) \quad (10)$$

where  $\tau_0 = 10^{-13}(1) \text{ s}$  and  $E_a = 0.48(8) \text{ eV}$ . The activation energy is a measure of the amount of energy necessary for the muon to activate out of an octahedral site and diffuse between O sites. The optical vibration frequency  $\nu_p$  for protons in the tetrahedral sites of  $\text{TiH}_2$  is  $3.3 \times 10^{13} \text{ s}^{-1}$ .<sup>12</sup> The muon's oscillation frequency in the octahedral sites should be close to this value. The vibration frequencies for the titanium atoms are about an order of magnitude slower. An attempt frequency for hopping should be multiplied by a factor representing the number of paths available for hopping, a number of order 6. We can therefore only conclude that the mechanism responsible for the activation of the muon out of the octahedral site is associated with the vibrations of the muon or hydride lattice atoms.

### III. Monte Carlo Simulations

The disagreement between activation energies measured by  $\mu$ SR and NMR has persisted for almost ten years with the one exception being the study of  $\text{VH}_{0.503}$ .<sup>6</sup> Richter et al.<sup>7</sup> proposed that the motion of the muon was limited by the availability of vacancies near the muon in  $\text{NbH}_x$  and  $\text{NbD}_x$  and that the field-correlation time,  $\tau_c$ , was a measure of the length of time for the field to change due to the motion of the muon in the dipolar fields generated by the niobium nuclei. The motion of the protons in this system primarily has the effect of providing vacancies near the site of the muon and will not contribute significantly to the field correlation for the muon in this system. However, this is not true for the  $\mu$ SR studies of  $\text{ZrH}_x$ <sup>6</sup>,  $\text{PdH}_x$ <sup>8</sup>,  $\text{TiH}_x$ <sup>1</sup>, and  $\text{YH}_x$ <sup>9</sup> since the dominant contribution to the dipolar field at the site of the muon is the sublattice of protons. This means that the motion of the protons changes the field at the site of the muon. In other words, the motion of the protons alone will produce a finite field-correlation time for a stationary muon. Since the muon is much lighter, and should be able to jump at a higher rate than a proton, the motion of the muon should be impeded by the motion of the hydrogen nuclei yielding an activation energy for the muon field-correlation time of the same order as that for protons. However, since the activation energies and prefactors were different for proton- and muon-field-correlation times,<sup>1</sup> we implemented Monte Carlo simulations to describe the effects of motion of the muon and the protons upon the muon field-correlation time.

Since the path for motion of vacancies (hydrogen atoms) in  $TiH_x$  is known to be between nearest-neighbor T sites (as determined by NMR),<sup>13</sup> we developed a model with four adjustable parameters:  $p$ ,  $p'$ ,  $p_{in}$ , and  $p_{out}$ , to describe the field-correlation time for the muon with the restriction that the motion of the muon be limited to nearest-neighbor jumping. The motion of the vacancies in the unperturbed lattice, i.e. not near a muon, occurs with some rate  $p$ . When the vacancy is next to the muon, the rate for the muon to move or the rate for the vacancy to move to the site of the muon is  $p'$ . This allows the muon jump rate to differ from the proton jump rate. Two other rates,  $p_{in}$  and  $p_{out}$ , have been added to account for the attraction or repulsion of vacancies due to the presence of the muon. These reflect a change in vacancy jump rate as the vacancy approaches the muon.  $p_{in}$  is the rate at which a second-nearest-neighbor vacancy to the muon will become a nearest neighbor.  $p_{out}$  is the rate at which a nearest-neighbor vacancy to the muon will become a second-nearest neighbor.

The  $9 \times 9 \times 9$  lattice used for the simulations had periodic boundary conditions which allowed particles to diffuse from one edge to the opposite edge. Initially, the muon was placed at the center of the lattice with seven ( $\approx 1\%$ ) vacancies randomly distributed. The direction of the external magnetic field was picked randomly with respect to the coordinate system of the lattice. The spins on the remaining lattice locations (excluding the positions of the vacancies) were randomly given orientations parallel or antiparallel to the field. After this was done, the

dipolar magnetic field due to the protons in the lattice at the site of the muon was calculated. Having done this, the vacancies were allowed to move. After each time step, the dipolar magnetic field at the site of the muon was computed. The total number of time steps was usually 3000-4000, which was large enough to determine the field-correlation time at the site of the muon. Each simulation produced the dot product of the dipolar magnetic field as a function of time with a unit vector in the direction of the external field  $\hat{B}_{\text{ext}}$

$$B(t) = \vec{B}_{\text{dip}}(t) \cdot \hat{B}_{\text{ext}} \quad (11)$$

The results of each simulation were then multiplied by the dot product of the dipolar magnetic field at time  $t=0$  dotted with a unit vector in the direction of the external magnetic field ( $B(0) = \hat{B}_{\text{dip}}(0) \cdot \hat{B}_{\text{ext}}$ ).  $\langle B(t)B(0) \rangle$ , which is used to calculate  $G(t)$ , was obtained by averaging  $B(t)B(0)$  over all simulations with the same values for the four parameters:  $p$ ,  $p'$ ,  $p_{\text{in}}$ , and  $p_{\text{out}}$ .

$$G(t) = \exp[-\gamma^2 \int_0^t (t-t') \langle B(t')B(0) \rangle dt'] \quad (12)$$

A field-correlation time,  $\tau_c$ , is defined such that  $\langle B(\tau_c)B(0) \rangle / \langle B(0)B(0) \rangle = 1/e$ .

In order to make the results independent of  $p$ ,  $\tau_c$  was multiplied by  $p$ . The results of the simulations are shown in Table I. The statistical error in these results is estimated to be of the order of five percent or less.

#### IV. High Temperature Motional Narrowing of the $\mu$ SR Signal

The results of the Monte Carlo simulations were given in terms of a  $p\tau_c$  product where  $p$  is the vacancy jump rate in an unperturbed lattice and  $\tau_c$  is the field-correlation time. In order to compare the data to the results of the simulations, we must multiply the muon field-correlation time by the vacancy jump rate.

The vacancy jump rate can be determined from the proton NMR data on  $\gamma$ -TiH<sub>x</sub> of Korn and Zamir<sup>12</sup> and of Bustard et al.<sup>13</sup> Korn and Zamir<sup>12</sup>, using Bloembergen, Purcell and Pound (BPP) theory, found that the proton field-correlation time is:

$$\tau_c = (\tau_0)/((2-x)/2)\exp[E_a/kT] \text{ s.} \quad (13)$$

Where  $\tau_0 = 2.8(5) * 10^{-14}$ , and  $E_a = 0.507(10)$  eV.

For proton-proton dipolar interactions, the mean dwell time at a site,  $\tau$ , (also known as the autocorrelation time) is approximately equal to  $2\tau_c$ . Since  $4p\tau c$  (where  $c$  is the vacancy concentration which is equal to  $(2-x)/2$ ) is of the order of 1 for an SCC lattice, then

$$p = (8\tau_0)^{-1}\exp[-E_a/kT] \text{ s}^{-1}. \quad (14)$$

Bustard et al.<sup>13</sup> state that BPP theory may not yield the correct values for the field-correlation time, because it is not dependent upon the type of lattice and does not provide for correlation effects between diffusing atoms. Instead of using BPP

theory, they used an independent spin-pair relaxation model to interpret their spin-lattice relaxation times,  $T_1$ . Their Monte Carlo model monitored the time evolution of a large number of spin pairs. Using the results of their simulations, they determined the mean dwell time for a proton at a site,  $\tau$ , from their  $T_1$  data and also from the  $T_1$  data of Korn and Zamir<sup>12</sup> and found

$$\tau = (9.3(6) * 10^{-15}) / (1/2(2-x)) \exp[0.555(7) \text{eV}/kT] \text{ s} \quad (15)$$

This yields a vacancy jump rate of

$$p = (2.7(2) * 10^{13}) \exp[-0.555(7) \text{eV}/kT] \text{ s}^{-1}. \quad (16)$$

Multiplying the vacancy jump rates obtained from both references by the muon field-correlation times for  $\text{TiH}_{1.97}$ , we obtain the  $p\tau_C$  product values shown in Table II. The proton hopping rates obtained by the later and more sophisticated work of Bustard et al.<sup>13</sup> are roughly half those of Korn and Zamir<sup>14</sup>.

The  $p\tau_C$  products obtained using either set of proton hopping rates are only constant below 500 K and rise to about twice their lower temperature values by 563 K. Naively, one would expect the vacancy hopping rates near the muon to be about equal to the rate further away:  $p_{\text{out}} = p_{\text{in}} = p$ ; and the muon to hop to a nearest neighbor vacancy at least as fast as a proton:  $p' \geq p$ . We see from a comparison of the tables this does not work for  $T > 500\text{K}$  for either set of proton hopping rates, and for those of Bustard et al. (Table II, column 2) at any temperature. An increase of

$p_{rC}$ , but with  $p' \geq p$  can be achieved by a reduction of the rate at which a vacancy hops to a nearest neighbor site, simulation 8 or 10,  $p_{in} = p/10$ , otherwise one must also reduce  $p'$ , simulation 7. A very dramatic increase in the rate of vacancy hopping away from a nearest neighbor site can increase  $p_{rC}$  moderately, simulation 5. However, if the results of Bustard et al. are used, we see that reducing the muon's motion alone ( $p' = 0$ , simulation 7) is not sufficient and the approach of a vacancy must be restricted,  $p_{in} < p$ , see simulations 7 - 12. The treatment by Bustard et al. was developed specifically for motion of the hydrogen nuclear spins on an SC lattice and would appear to be better suited for extraction of a proton autocorrelation time from  $T_1$  data compared to BPP theory. However, using an independent spin-pair relaxation model to obtain the vacancy jump rate requires that the muon affect the motion of the nearest-neighbor protons.

A vacancy to muon-site hopping rate less than that for a proton implies the involvement of some other mechanism. This may also be related to the requirement that  $p_{in}$  be reduced relative to  $p$ . If the nearest-neighbor hydrogens are bound to the muon by an excess of 0.1 eV this would reduce  $p_{in}$  sufficiently and possibly force muon hopping to next-nearest-neighbor sites, which are further apart and would hence reduce the prefactor by an order of magnitude.

## V. Conclusions

We have reanalyzed the  $\text{TiH}_{1.99}$  data taken near room temperature by Kossler et al.<sup>1</sup> and have shown that they can be fit to a model with many shallow traps and a low concentration of deeper traps for the muon. We find that the mechanism responsible for the activation of the muon out of the shallow trap (O site) is associated with the vibration of the hydrogen sublattice. Secondly, a method of simulating the effect of the motion of protons and the muon on the field-correlation time is presented and applied to the motional narrowing of the  $\mu\text{SR}$  signal in  $\text{TiH}_{1.97}$  for temperatures near 500 K. The conclusions from the comparison of the  $\rho_{\text{FC}}$  obtained from the data and from the simulations are dependent on the method of analysis to obtain an autocorrelation time for the proton from proton NMR data for  $\gamma\text{-TiH}_x$ . Using the results of Korn and Zamir<sup>12</sup>, we find that the motion of the muon decreases with respect to the motion of the proton as the temperature increases. Using the results of Bustard et al.<sup>13</sup>, we find that a stationary muon does not explain the results of Kossler et al.<sup>1</sup> and that the presence of the muon inhibits the motion of the nearest-neighbor protons. It would seem that the method used by Bustard et al.<sup>13</sup> is better suited for analysis of proton  $T_1$  data for  $\gamma\text{-TiH}_x$ , but the model needed to describe the results of  $\mu\text{SR}$  experiments is more complicated than the model developed using BPP theory employed by Korn and Zamir<sup>12</sup> to derive the vacancy jump rate. We believe that the conclusions reached for  $\text{TiH}_{1.97}$  are also valid for  $\text{TiH}_{1.83}$ , since the proton and muon correlation times scale inversely with the vacancy concentration. We also

believe that these conclusions are valid for other FCC metal hydrides, i.e.,  $ZrH_x$  and  $YH_x$ .

#### Acknowledgements

The present work is supported by the National Science Foundation under Grant No. DMR-8503223, by NASA under Grant NAG-1-416, and by the Division of Materials Science of the U. S. Department of Energy under Contract No. AC02CH00016.

## References

1. W. J. Kossler, H. E. Schone, K. Petzinger, B. Hitti, J. R. Kempton, E. F. W. Seymour, C. E. Stronach, W. F. Lankford and J. J. Reilly, *Hyp. Int.* 31, 235 (1986).
2. G. Alefeld and J. Völkl, in *Hydrogen in Metals I* edited by G. Alefeld and J. Völkl (Springer-Verlag, Berlin, 1978).
3. R. M. Cotts, in *Hydrogen in Metals I* edited by G. Alefeld and J. Völkl (Springer-Verlag, Berlin, 1978).
4. K. W. Kehr, in *Hydrogen in Metals I*, edited by G. Alefeld and J. Völkl (Springer-Verlag, Berlin, 1978) and references therein.
5. Y. Fukai, K. Kubo, and S. Kazama, *Z. Phys. Chem.* 115, 181 (1979).
6. M. Doyama, R. Nakai, R. Yamamoto, Y.J. Uemura, T. Yamazaki, Fukai and T. Suzuki, *Hyp. Int.* 8, 711 (1981).
7. D. Richter, R. Hempelmann, O. Hartmann, E. Karlsson, L. O. Norlin, S. F. J. Cox and R. Kutner, *J. Chem. Phys.* 79, 4564 (1983).
8. F. N. Gygax, A. Hintermann, W. Rüegg, A. Schenck, W. Studer, A. J. Van der Wal, J. H. Brewer, F. Stucki and L. Schlapbach, *Hyp. Int.* 17-19, 267 (1984).
9. W. J. Kossler, H. E. Schone, J. R. Kempton, B. Hitti, C. E. Stronach, G. A. Styles and E. F. W. Seymour, *J. Less-Common Met.* 129, 327 (1987).
10. C. Boekema, R. H. Heffner, R. L. Hutson, M. Leon, M. Schil-laci, W. J. Kossler, M. Numan and S. A. Dodds, *Phys. Rev. B* 26, 2341 (1982).
11. W. J. Kossler, A. T. Fiory, W. F. Lankford, J. Lindemuth, K. G. Lynn, S. Mahajan, R. P. Minnich, K. G. Petzinger and C. E. Stronach, *Phys. Rev. Let.* 41, 1558 (1978).
12. C. Korn and D. Zamir, *J. Phys. Chem. Solids* 31, 489 (1970).
13. L. D. Bustard, R. M. Cotts, and E. F. W. Seymour, *Z. Phys. Chem.* 115, 247 (1979).
14. K. G. Petzinger, *Phys. Rev. B* 26, 6530 (1982).

TABLE I  $p\tau_c$  products from Monte Carlo simulations.  $p$  is the vacancy hopping rate far from the muon,  $p'$  is the rate at which the muon moves to a nearest-neighbor vacancy,  $p_{in}$  is the vacancy rate for next-nearest-neighbor to nearest-neighbor jumps,  $p_{out}$  is the rate for the converse process of  $p_{in}$ , and  $\tau_c$  is the field correlation time for the muon.

---



---

<u>Simulation#</u>	<u>Probabilities</u>	<u><math>p\tau_c</math></u>
01	$p'=p_{out}=p, p_{in}=10p$	6
02	$p_{in}=p_{out}=p, p'=10p$	12
03	$p'=p_{in}=p, p_{out}=p/100$	13
04	$p'=p_{in}=p_{out}=p$	23
05	$p'=p_{in}=p, p_{out}=10p$	32
06	$p_{in}=p_{out}=p, p'=p/100$	49
07	$p_{in}=p_{out}=p, p'=0$	52
08	$p_{out}=p, p_{in}=p/10, p'=10p$	61
09	$p_{in}=p, p_{out}=p/100, p'=0$	61
10	$p_{out}=p'=p, p_{in}=p/10$	98
11	$p_{out}=p'=p, p_{in}=p/100$	450
12	$p_{out}=p, p_{in}=p/100, p'=0$	452

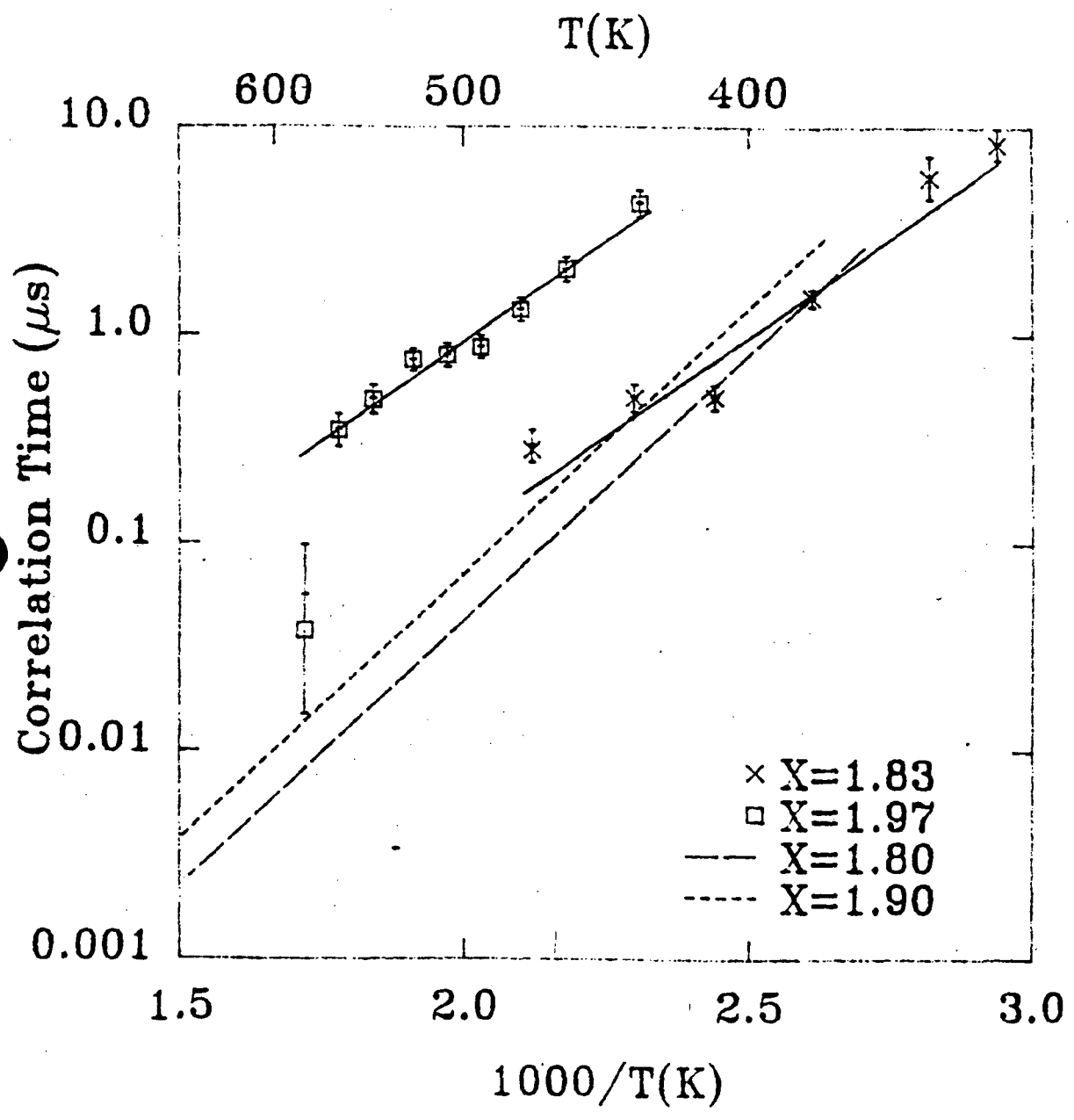
---

TABLE II.  $p r_c$  products for  $TiH_{1.97}$  data.

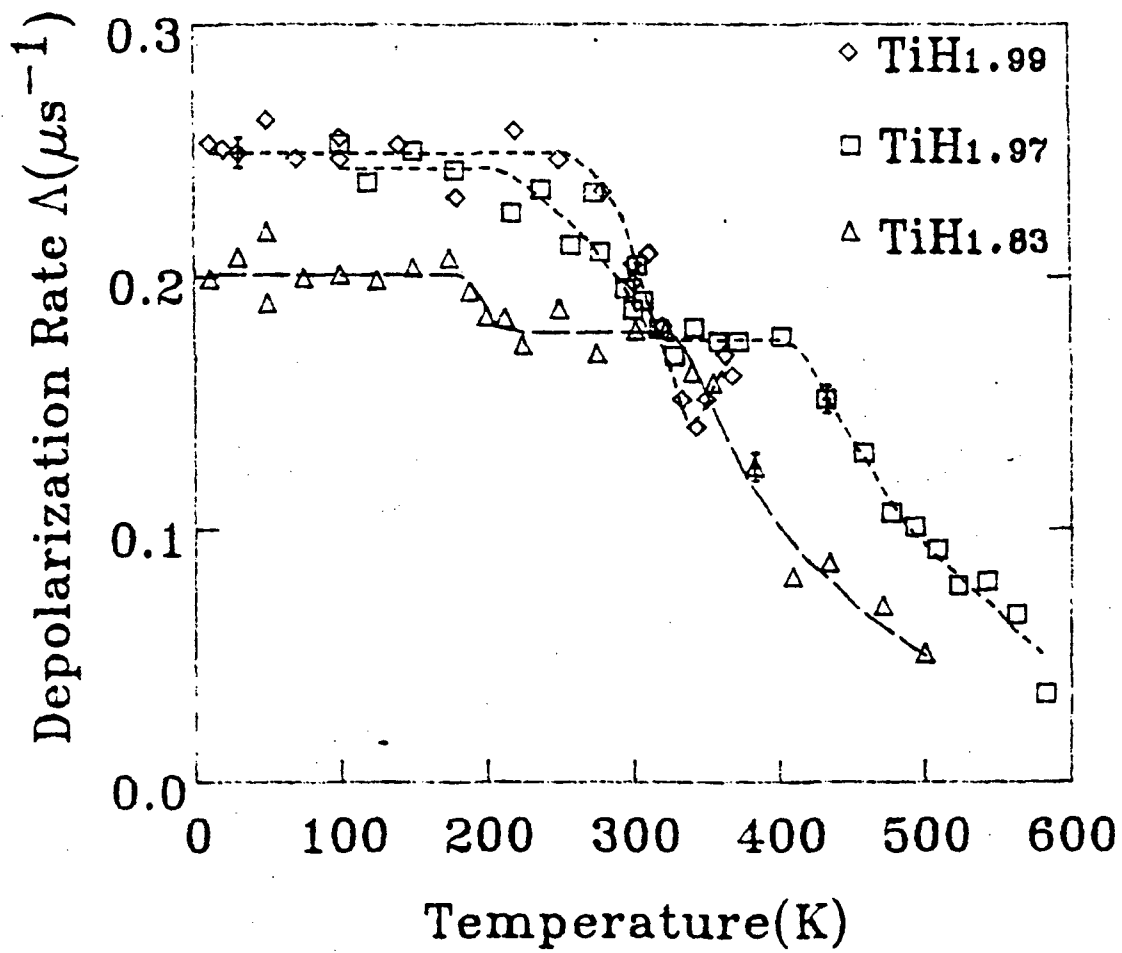
<u>T(K)</u>	<u><math>r_c(\mu s)</math></u>	<u><math>p(K\&amp;Z)r_c</math></u>	<u><math>p(B)r_c</math></u>
432	4.3(7)	24(9)	39(10)
458	2.1(3)	25(9)	44(11)
477	1.3(2)	26(9)	49(11)
493	0.9(1)	26(9)	50(11)
508	0.8(1)	34(11)	68(15)
523	0.8(1)	45(14)	93(20)
543	0.49(9)	43(15)	93(22)
563	0.35(7)	45(16)	101(26)
583	0.04(6)	7(11)	16(26)

K&Z indicates that the vacancy hopping rate has been taken from Korn and Zamir<sup>12</sup>.

B indicates that the rate is from Bustard et al.<sup>13</sup>.



24



APPENDIX H

N88-24248

56-76

142721

P-13

Search for Bound States of the  $\eta$ -Meson in Light Nuclei

R. E. Chrien, S. Bart, P. Pile, R. Sutter, N. Tsoupas  
Brookhaven National Laboratory, Upton, NY 11973

H. O. Funsten, J. M. Finn, C. Lyndon, V. Punjabi, C. F. Perdrisat /  
College of William and Mary, Williamsburg, VA 23185

B. J. Lieb  
George Mason University, Fairfax, VA 22030

T. Kishimoto\*  
University of Houston, Houston, TX 77004

L. C. Liu, R. Estep, B. Dropesky  
Los Alamos National Laboratory, Los Alamos, NM 87545

C. E. Stronach  
Virginia State University, Petersburg, VA 23803

R. L. Stearns  
Vassar College, Poughkeepsie, NY 12601

Abstract

A search for nuclear-bound states of the  $\eta$  meson has been carried out. Targets of lithium, carbon, oxygen, and aluminum were placed in a  $\pi^+$  beam at 800 MeV/c. A predicted  $\eta$  bound state in  $^{15}\text{O}^*$  ( $E_x \approx 540$  MeV) with a width of  $\approx 9$  MeV was not observed. A bound state of a size 1/3 of the predicted cross section would have been seen in this experiment at a confidence level of  $3\sigma$  ( $P > 0.9987$ ).

\*Now at Osaka University, Japan

ORIGINAL PAGE IS  
OF POOR QUALITY

This paper describes a search for a novel nuclear excitation involving the creation of a bound  $\eta$ -meson in the nuclear medium. The concept is similar in spirit to a number of ideas which have been recently vigorously pursued. Some familiar examples are  $\Lambda$  hypernuclear states,  $\Sigma$ -hypernuclear states, antiprotonic nuclear states, and various dibaryon resonances. In each case an attractive particle-nucleus potential is required and some mechanism to inhibit the decay process, such as strangeness conservation in the case of the  $\Lambda$ .

Several suggestions of the existence of bound states of the  $\eta$ -meson in a wide range of nuclei have recently been published<sup>1-3</sup>. The suggestions of this novel nuclear excitation are based on bound state formation through the attractive  $N$ - $\eta$  channel of the  $N^*(1535)$ , where  $N^*(1535)$  is the  $(\pi N)$  resonance with  $(I, J^\pi) = (1/2, 1/2^-)$  and mass  $1535 \text{ MeV}/c^2$ . This resonance dominates  $\eta$  production near threshold. Bhalerao and Liu<sup>4</sup> have shown, by a coupled-channel analysis, that the low-energy  $\eta N$  interaction is attractive with a scattering length of  $(0.28 + 0.202i)$  fermi. The attractive interaction is a consequence of the threshold being below the  $N^*(1535)$  resonance.

Liu and his collaborators have examined the consequences of this attractive interaction in the formation of a bound- $\eta$  state as a function of mass number. Their study indicates that nuclear bound states could exist for mass numbers larger than  $A \approx 10$ . At low mass numbers, only s-state bound  $\eta$ 's are predicted. At larger mass numbers, p- and d-states could become bound. Both binding energies and widths increase with  $A$ . The optimum case, in their analysis, is  ${}_{\eta}^{15}\text{O}$ , formed from the  $(\pi^+, p)$  reaction on  ${}^{16}\text{O}$  at a momentum near  $740 \text{ MeV}/c$ .<sup>3</sup> At an angle near  $15^\circ$ , the momentum transfer is favorable for the transition involving the conversion of p-shell neutron to an s-shell  $\eta$ . For higher mass numbers, the increase in predicted width would make this excitation more difficult to see over the continuum  $(\pi^+, p)$  background which is present.

An experiment to test these predictions was devised with the positive pion beam available at the Low-Energy Separated Beam I at the Brookhaven Alternating Gradient Synchrotron (AGS), and the Moby Dick Spectrometer. The experimental arrangement is virtually identical with that used for the production and measurement of hypernuclei, and it has been described in detail in a number of publications (see Ref. 5 and related references). The only differences involve the selection of pions, rather than kaons, in the incident particle channel and protons in the exiting particle channel.

The spectrometer was set at  $15^\circ$  to be near the maximum for bound eta production as predicted in the analysis of Liu and Haider<sup>1,3</sup>. For example, reference 3 predicts the production of an  $\eta$  excitation of width of 9 MeV (FWHM) and a peak cross section of about 30  $\mu\text{b}/\text{sr-MeV}$ , for an incident pion momentum of 800 MeV/c on an  $^{16}\text{O}$  target. The peak would appear near zero binding energy in the ( $^{15}\text{O}+\eta$ ) missing mass spectrum corresponding to the emission of protons with 248 MeV kinetic energy in the lab frame, and an excitation of 540 MeV in the  $^{15}\text{O}$  system.

Four targets were selected for examination; the target parameters are listed in Table I. The oxygen target was in the form of water. For lithium, no  $\eta$ -bound states are predicted, while for carbon the binding is predicted to be marginal. Oxygen is expected to display the largest bound state cross section; for larger A the cross sections are smaller, while the widths grow larger.

To confirm a cross section scale and to measure a spectrometer momentum acceptance function, the reaction  $p(\pi^+,p)\pi^+$  was measured for a  $\pi^+$  momentum of

ORIGINAL PAGE IS  
OF POOR QUALITY

525 MeV/c. This reaction has been measured by the Leningrad group of Gordeev et al.<sup>6</sup>, and their reported cross sections were in reasonable agreement ( $\approx 20\%$ ) with our measurements. To establish the acceptance function, the nominal momentum setting of the proton spectrometer was varied from 620 to 780 MeV/c, and the strength of the observed  $\pi^+$  missing mass peak was used to determine the acceptance. It was desirable to limit the spectrometer acceptance correction to no more than 30% of the central value over the entire spectrum. With this criterion, an acceptance range of  $\approx 80$  MeV/c was obtainable; i.e., the relative acceptance is everywhere larger than 0.7 throughout the range. To obtain a sufficiently broad range in outgoing proton momenta, overlapping runs were taken for spectrometer central values of 657, 700, and 740 MeV/c.

The spectrometer resolution was measured by analyzing (p,p') events for  $^{12}\text{C}$ , recorded simultaneously with the  $(\pi^+,p)$  events. The missing mass resolution was studied in two separate ways: by using TRANSPORT<sup>7</sup> matrix elements to calculate the particle momenta, and also by using the program RAYTRACE<sup>8</sup>, which includes magnetic corrections to all orders. The spectrometer resolution was measured to be 4 MeV (FWHM) using the TRANSPORT analysis and 2.5 MeV (FWHM) using RAYTRACE. For either mode of analysis, the resolution is sufficient to detect the predicted  $\eta$ -states without serious resolution broadening of the peak.

These (p,p') studies also serve to confirm the energy scale and the energy losses in the target and beam windows of the experiment.

The results of the experiment on the 4 targets are shown in the composite diagram of Fig. 1. The inclusive proton spectra of this experiment show a qualitative similarity to recent  $(\bar{p},p)$  reaction studies on various nuclei by Garreta et al.<sup>9</sup> We know of no comparable  $(\pi^+,p)$  data at these pion energies. The data for each target show a smooth  $(\pi^+,p)$  cross section down to an energy corresponding to the  $\eta$  production threshold. At lower energies, the cross

ORIGINAL PAGE IS  
OF POOR QUALITY

525 MeV/c. This reaction has been measured by the Leningrad group of Gordeev et al.<sup>6</sup>, and their reported cross sections were in reasonable agreement ( $\approx 20\%$ ) with our measurements. To establish the acceptance function, the nominal momentum setting of the proton spectrometer was varied from 620 to 780 MeV/c, and the strength of the observed  $\pi^+$  missing mass peak was used to determine the acceptance. It was desirable to limit the spectrometer acceptance correction to no more than 30% of the central value over the entire spectrum. With this criterion, an acceptance range of  $\approx 80$  MeV/c was obtainable; i.e., the relative acceptance is everywhere larger than 0.7 throughout the range. To obtain a sufficiently broad range in outgoing proton momenta, overlapping runs were taken for spectrometer central values of 657, 700, and 740 MeV/c.

The spectrometer resolution was measured by analyzing (p,p') events for  $^{12}\text{C}$ , recorded simultaneously with the  $(\pi^+,p)$  events. The missing mass resolution was studied in two separate ways: by using TRANSPORT<sup>7</sup> matrix elements to calculate the particle momenta, and also by using the program RAYTRACE<sup>8</sup>, which includes magnetic corrections to all orders. The spectrometer resolution was measured to be 4 MeV (FWHM) using the TRANSPORT analysis and 2.5 MeV (FWHM) using RAYTRACE. For either mode of analysis, the resolution is sufficient to detect the predicted  $\eta$ -states without serious resolution broadening of the peak.

These (p,p') studies also serve to confirm the energy scale and the energy losses in the target and beam windows of the experiment.

The results of the experiment on the 4 targets are shown in the composite diagram of Fig. 1. The inclusive proton spectra of this experiment show a qualitative similarity to recent  $(\bar{p},p)$  reaction studies on various nuclei by Garreta et al.<sup>9</sup> We know of no comparable  $(\pi^+,p)$  data at these pion energies. The data for each target show a smooth  $(\pi^+,p)$  cross section down to an energy corresponding to the  $\eta$  production threshold. At lower energies, the cross

ORIGINAL PAGE IS  
OF POOR QUALITY

section appears to increase, and it is plausible to attribute this increase to the quasi-free  $\eta$  production process. For the aluminum, oxygen, and possibly carbon cases an eta peak would be expected to appear near the position of the arrow.

The sensitivity of this experiment to narrow  $\eta$  bound-state peaks is obviously compromised by the large proton continuum background observed in this experiment. This background is presumably attributable to nuclear protons ejected by the incident pions through various processes, including quasi-free knockout, multiple pion and proton scattering, and pion absorption. To establish the experimental sensitivity quantitatively, a statistical analysis was carried out in detail. The analysis was made on data that were not corrected for momentum acceptance, since the correction process increased the spread of the data points significantly. Fluctuations about a polynomial fit to the uncorrected data were analyzed with a standard least squares fitting code.

The quantitative statement of the experimental sensitivity, based on the largest observed fluctuation in the data, is the following: the detection of a peak with a full-width at half maximum of 9 MeV in the  $^{16}\text{O}$  data occurs at a confidence level of  $3\sigma$  (0.9987) for a peak height of 8.7  $\mu\text{b}/\text{sr}/\text{MeV}$ . This size is about one-third of the prediction of Ref. 3. The  $^{16}\text{O}$  target was predicted in Ref. 3 to be the most favorable case, i.e., the one displaying the largest cross section. Similar sensitivities obtain for the lithium and carbon cases, while for aluminum the size of the fluctuations, due to a poorer statistical accuracy, preclude any strong statements.

It is interesting to remark on the similarities of the spectra shown in Fig. 1 with the spectra obtained in the experiment of Garreta<sup>9</sup>--both of which experiments were designed to search for narrow states located near the onset of a quasi-free process. In the latter the search is for  $\bar{p}$  states, while in our

ORIGINAL PAGE IS  
OF POOR QUALITY

work, we are searching for a structure due to bound  $\eta$  states.

The  $(\bar{p}, p)$  process is thought to proceed via the annihilation of the  $\bar{p}$  with a target nucleon to produce, on average, 5 pions which subsequently interact with the A-1 target nucleons and eject protons. Thus the subsequent stages of the process are similar to the  $(\pi^+, p)$  reaction. Reference 9 documents the fact that over a very wide range of proton momenta, the cross section has a Maxwellian shape:

$$d^2\sigma/d\Omega dE = C(E)^{1/2} \exp\{-E/T\}$$

where E represents proton kinetic energy.

We adopted the same parameterization to characterize the  $(\pi^+, p)$  data. For the fitting procedure, it was necessary to exclude the  $\eta$  quasi-free region; hence only data outside the allowed kinematical range of  $\eta$  production was used. The resulting fits were then extrapolated into the  $\eta$  quasi-free region, these fits are indicated in Fig. 1. We believe that the obvious excess which occurs near the onset of the  $\eta$  threshold is attributed to  $\eta$  quasi-free processes.

An expanded region near the  $\eta$  threshold is shown in Fig. 2 for the oxygen target. To indicate the various reaction mechanisms more explicitly, three curves are shown: the dashed curve is the Maxwellian fit to the  $(\pi^+, p)$  inclusive process, the solid curve shows an estimate of the quasi-free  $\eta$  production added to the Maxwellian, and the dotted curve shows the p-shell bound eta state predicted by Liu and Haider<sup>1,3</sup>. It should be clear from the figure that a peak of the predicted size would be visible in the experiment; it is not seen.

The size of the quasi-free production observed in the <sup>16</sup>O data is roughly in line with the observations of Peng and collaborators<sup>10</sup> at a somewhat lower beam momentum of 680 MeV/c. An estimate of the magnitude of the expected

ORIGINAL PAGE IS  
OF POOR QUALITY

quasi-free eta production was based on the elementary cross sections of Litchfield et al.<sup>11</sup> and of Brown et al.<sup>12</sup> (the latter for the charge conjugate ( $\pi^-$ ,n) reaction). The shape of the onset of the quasi-free process near threshold was taken from Ref. 3, and that result was arbitrarily normalized to our data as shown in Fig. 1. From this normalization, a result for the effective number of scatterers, defined as,

$$N_{\text{eff}} = \frac{d\sigma(\text{nuclear})}{d\sigma(\text{elementary})}$$

can be obtained. The preliminary estimate of the quasi-free cross section, derived from the fit of Fig. 2 and integrated over the spectrum shape presented by Ref. 3 leads to a value  $d\sigma/d\Omega$  (qf)  $\approx$  150  $\mu\text{b}$  as compared to a value 191  $\mu\text{b}$  derived from Ref. 11. We estimate therefore that  $N_{\text{eff}}$  is of the order of unity ( $\approx$ 0.8). This is quite comparable to the value characteristic of hypernuclear cross sections and an order of magnitude higher than  $N_{\text{eff}}$  deduced from ( $\bar{p}$ ,p) nuclear interactions.

In summary, the search for a narrow  $\eta$ -nuclear bound state has produced negative results. A peak one-third the size predicted would have been seen in oxygen at a confidence level of 3 $\sigma$ . The conclusion is either that widths for such excitations are much larger than predicted, or that the production cross sections are much smaller than predicted, or both.

The authors express their appreciation to the AGS technical staff and to the BNL Medium Energy Group support staff consisting of E. Meier, A. Minn, and J. Rutherford. This research has been performed under the following grants: DE-AC02-76CH00016 (USDOE), DE-AS05-76ER0 (USDOE), PHY-8509880-05 (NSF), and NAG-1-416 (NASA).

ORIGINAL PAGE IS  
OF POOR QUALITY

References

1. Q. Haider and L. C. Liu, Phys. Lett. 172B, 257 (1986); 174B, 465 (E) (1986).
2. G. L. Li, W. K. Cheng, T. T. S. Kuo, Phys. Lett. 195B, 515 (1987).
3. L. C. Liu and Q. Haider, Phys. Rev. C34, 1845 (1986).
4. R. S. Bhalerao and L. C. Liu, Phys. Rev. Lett. 54, 865 (1985).
5. E. C. Milner et al., Phys. Rev. Lett. 54, 1237 (1980).
6. V. A. Gordeev et al., Nucl. Phys. A364, 408 (1981).
7. Karl Brown et al., CERN Report 80-04 (1980).
8. S. Kowalski and H. Enge, Proceedings of the International Conference on Magnet Technology, Hamburg, 366 (1970), unpublished), and H. Enge (private communication).
9. D. Garreta et al., Phys. Lett. 150B, 95 (1985); D. Garreta et al., Nucl. Phys. A470, 445 (1987).
10. J. C. Peng in "Hadronic Probes and Nuclear Interactions", AIP Conf. Proc. 133m 255 (1985).
11. P. J. Litchfield, Phys. Rev. 183, 1152 (1969).
12. R. M. Brown et al., Nucl. Phys. B153, 89 (1979).

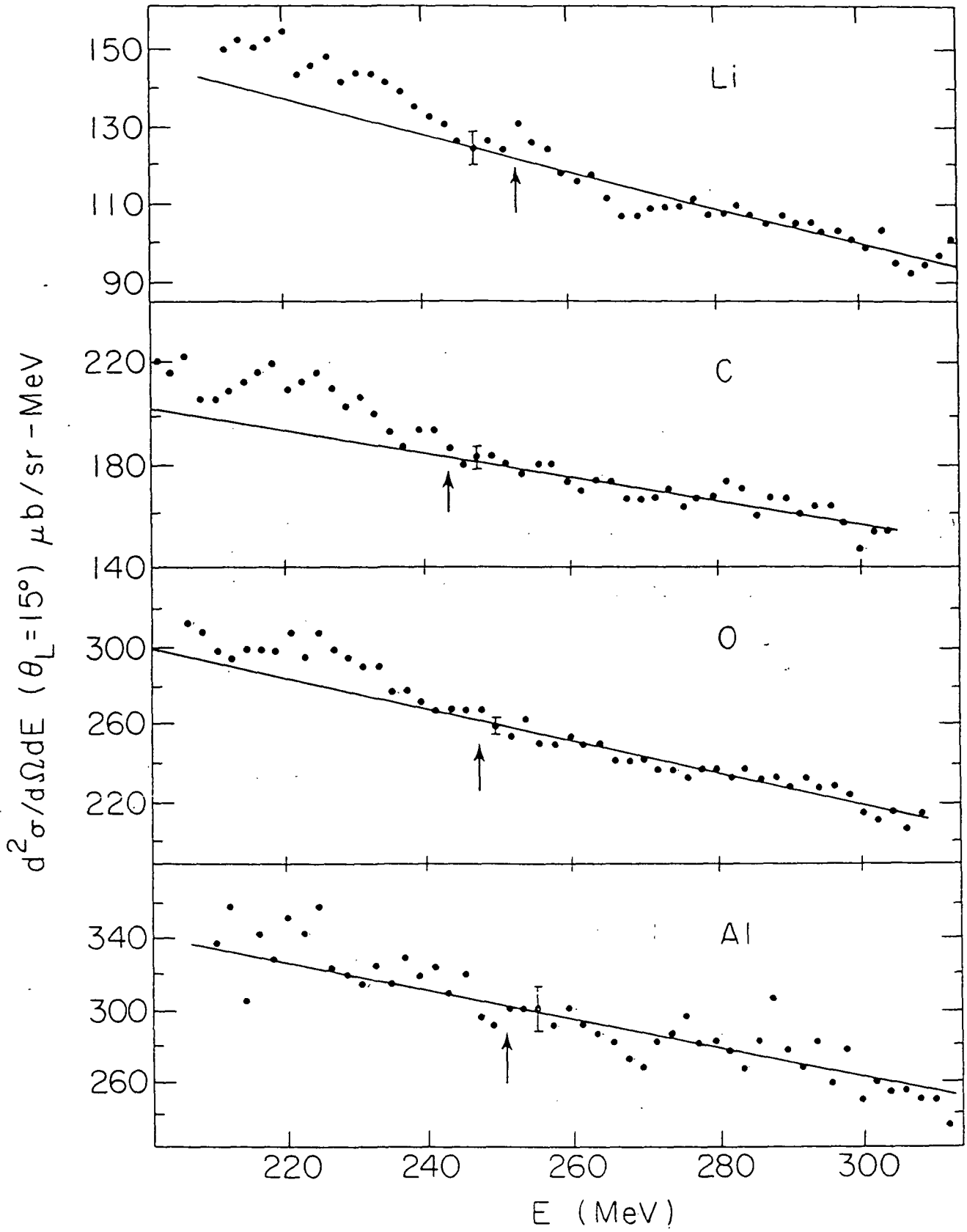
1. The proton kinetic energy spectra obtained for the targets examined in this experiment at 800 MeV/c incident  $\pi^+$ . In each case, a Maxwellian function was fit to the  $(\pi^+, p)$  inclusive proton energy above the eta production threshold. The arrows indicate that threshold for each target. The error bar shown indicates the standard deviation for a typical datum near threshold.
2. The region of the oxygen spectrum in which an  $\eta$ -bound state would appear is shown in this figure. The dashed curve shows the extrapolated Maxwellian fit to the inclusive  $(\pi, p)$  background, and the solid curve shows the quasi-free  $\eta$ -production added to the  $(\pi, p)$  background. The dotted curve indicates a state in which a  $p_{1/2}$  shell neutron has been transformed into a bound  $\eta$ , with the size, width and binding predicted by ref. 3. The data are clearly inconsistent with that prediction.

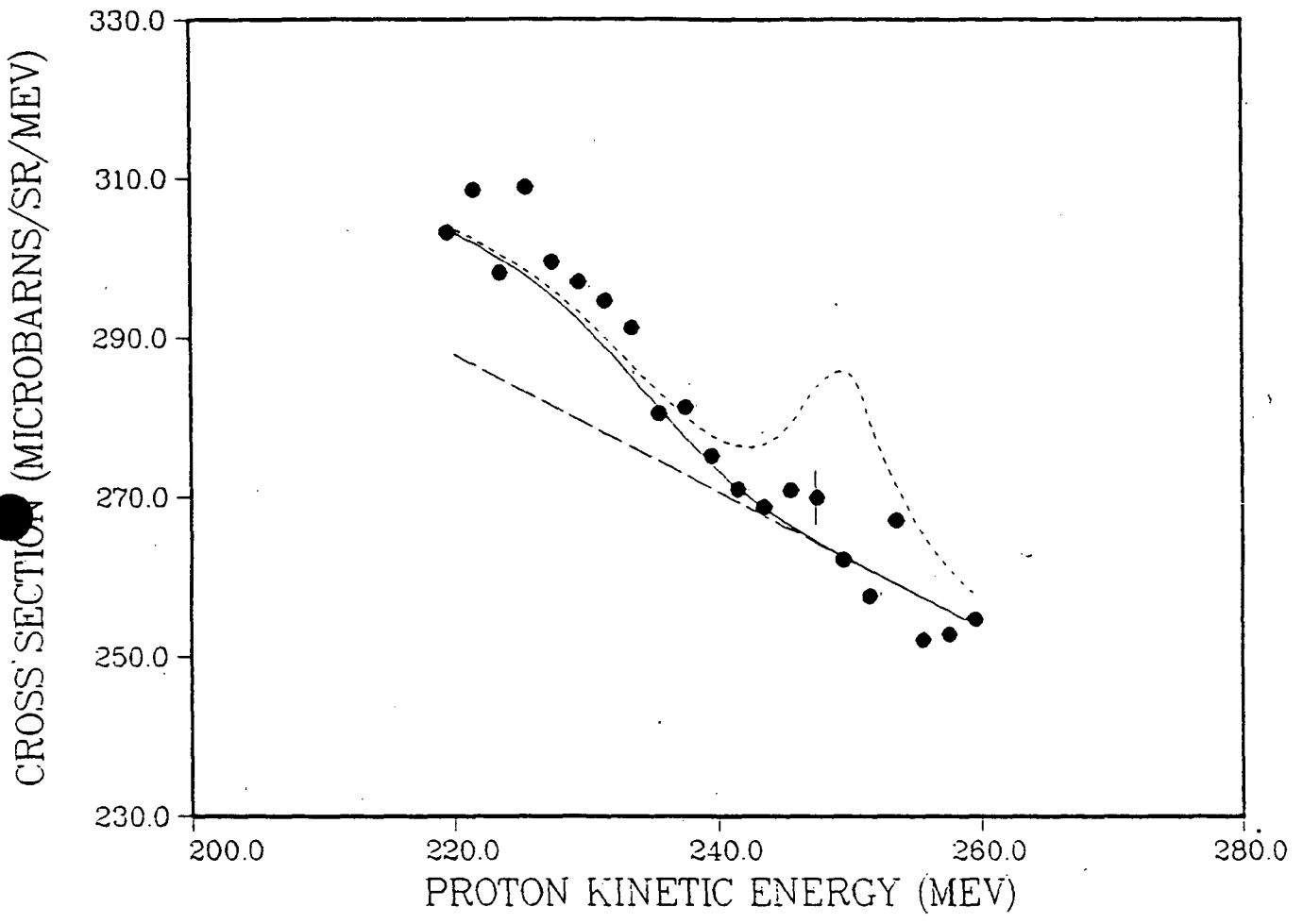
Table 1. The target thicknesses and the total dead-time-corrected pion irradiations for the spectra obtained in this experiment are indicated.

Target	Thickness (gm/cm <sup>2</sup> )	Dead-Time-Corrected Pion Irradiation
Li	2.23	$2.92 \times 10^{10}$
C	1.50	$2.99 \times 10^{10}$
Water	2.15	$4.57 \times 10^{10}$
Al	2.03	$1.66 \times 10^{10}$
Polyethylene	2.15 (calibration)	$1.40 \times 10^{10}$

ORIGINAL PAGE IS  
OF POOR QUALITY

ORIGINAL PAGE IS  
OF POOR QUALITY





END

DATE

AUG. 23, 1988